

# A new basal ornithopod dinosaur from the Lower Cretaceous of China

Yuqing Yang<sup>1, 2, 3, 4</sup>, Wenhao Wu<sup>5, 6</sup>, Paul-Emile Dieudonné<sup>7</sup>, Pascal Godefroit<sup>Corresp. 8</sup>

<sup>1</sup> College of Paleontology, Shenyang Normal University, Shenyang, Liaoning, China

<sup>2</sup> College of Resources and Civil Engineering, Northeastern University, Shenyang, Liaoning, China

<sup>3</sup> Key Laboratory for Evolution of Past Life and Change of Environment, Province of Liaoning, Shenyang University, Shenyang, Liaoning, China

<sup>4</sup> Key Laboratory for Evolution of Past Life in Northeast Asia, Ministry of Natural Resources, Shenyang University, Shenyang, Liaoning, China

<sup>5</sup> Key Laboratory for Evolution of Past Life and Environment in Northeast Asian, Jilin University (吉林大学), Changchun, Jilin, China

<sup>6</sup> Research Center of Paleontology and Stratigraphy, Jilin University (吉林大学), Changchun, Jilin, China

<sup>7</sup> Instituto de Investigación en Paleobiología y Geología, CONICET, Universidad Nacional de Río Negro, Río Negro, Argentina

<sup>8</sup> Directorate 'Earth and History of Life', Royal Belgian Institute of Natural Sciences, Brussels, Belgium

Corresponding Author: Pascal Godefroit

Email address: Pascal.Godefroit@naturalsciences.be

A new basal ornithopod dinosaur, based on two subcomplete articulated skeletons, is reported from the Lujiatun Beds (Yixian Fm, Lower Cretaceous) of western Liaoning Province (China). Some of the diagnostic features of *Changmiania liaoningensis* nov. gen. nov. sp. are tentatively interpreted as adaptations to a fossorial behavior, including: fused premaxillae; nasal laterally expanded, overhanging the maxilla; shortened neck formed by only six cervical vertebrae; elongated sacrum formed by seven vertebrae; neural spines of the sacral vertebrae completely fused together, forming a craniocaudally-elongated continuous bar; fused scapulocoracoid with prominent scapular spine; and paired ilia symmetrically inclined dorsomedially, partially covering the sacrum in dorsal view. A phylogenetic analysis places *Changmiania liaoningensis* as the most basal ornithopod dinosaur described so far. It is tentatively hypothesized that both *Changmiania liaoningensis* specimens were suddenly entrapped in a collapsed underground burrow while they were resting, which would explain their perfect lifelike postures and the complete absence of weathering and scavenging traces. However, further behavioural inference remains problematic, because those specimens lack extensive sedimentological and taphonomic data, as it is also the case for most specimens collected in the Lujiatun Beds so far.

# A new basal ornithopod dinosaur from the Lower Cretaceous of China

Yang Yuqing<sup>1-4</sup>, Wu Wenhao<sup>5-6</sup>, Paul-Emile Dieudonné<sup>7</sup>, and Pascal Godefroit<sup>8</sup>

1. College of Resources and Civil Engineering, Northeastern University, Shenyang, Liaoning, China

2. College of Paleontology, Shenyang Normal University, Shenyang, Liaoning, China

3. Key Laboratory for Evolution of Past Life and Change of Environment, Province of Liaoning, Shenyang, Liaoning, China

4. Key Laboratory for Evolution of Past Life in Northeast Asia, Ministry of Natural Resources, Shenyang, Liaoning, China

5. Key Laboratory for Evolution of Past Life and Environment in Northeast Asian (Jilin University), Ministry of Education, Changchun, Jilin, China

6. Research Center of Paleontology and Stratigraphy, Jilin University, Changchun, Jilin, China

7. CONICET, Universidad Nacional de Río Negro. Instituto de Investigación en Paleobiología y Geología, Río Negro, Argentina

8. Royal Belgian Institute of Natural Sciences, Directorate 'Earth & History of Life', Brussels, Belgium

**Corresponding author:**

**Pascal Godefroit**

**Email address: [Pascal.Godefroit@naturalsciences.be](mailto:Pascal.Godefroit@naturalsciences.be)**

# Abstract

A new basal ornithopod dinosaur, based on two subcomplete articulated skeletons, is reported from the Lujiatun Beds (Yixian Fm, Lower Cretaceous) of western Liaoning Province (China). Some of the diagnostic features of *Changmiania liaoningensis* nov. gen. nov. sp. are tentatively interpreted as adaptations to a fossorial behavior, including: fused premaxillae; nasal laterally expanded, overhanging the maxilla; shortened neck formed by only six cervical vertebrae; elongated sacrum formed by seven vertebrae; neural spines of the sacral vertebrae completely fused together, forming a craniocaudally-elongated continuous bar; fused scapulocoracoid with prominent scapular spine; and paired ilia symmetrically inclined dorsomedially, partially covering the sacrum in dorsal view. A phylogenetic analysis places *Changmiania liaoningensis* as the most basal ornithopod dinosaur described so far. It is tentatively hypothesized that both *Changmiania liaoningensis* specimens were suddenly entrapped in a collapsed underground burrow while they were resting, which would explain their perfect lifelike postures and the complete absence of weathering and scavenging traces. However, further behavioural inference remains problematic, because those specimens lack extensive sedimentological and taphonomic data, as it is also the case for most specimens collected in the Lujiatun Beds so far.

**Subjects** Paleontology, Taxonomy

**Keywords** Dinosauria, Ornithopoda, Lower Cretaceous, Yixian Formation, Liaoning Province

# Introduction

The Lujiatun Beds of the Yixian Formation are the lowermost fossil-bearing horizon of the Jehol Group in western Liaoning Province, China (He et al., 2006). Thousands of perfectly preserved vertebrate fossils have been unearthed from this horizon, including lizards, mammals and dinosaurs. Unlike in other horizons from the Jehol Biota, the Lujiatun fossils are preserved in three dimensions, revealing unique behaviour information, such as parental care (Meng et al., 2004) and sleeping posture (Xu and Norell, 2004) of dinosaurs, and mammals eating dinosaurs (Hu et al., 2005). Those fossils are preserved in 5 to 20 meters thick tuffs exposed close to the Lujiatun Village, Shanyuan, Beipiao City. <sup>40</sup>Ar/<sup>39</sup>Ar dating of ash from the Lujiatun beds interbedded with the fossiliferous layers shows that the Lujiatun specimens are Barremian (123.2±1.0 Ma) in age (He et al., 2006). It has been hypothesized that the Lujiatun fauna was killed catastrophically by lahar from a nearby shield volcano (He et al., 2006; Zhao et al., 2007). A wide variety of theropod dinosaurs has been discovered in the Lujiatun Beds, including the tyrannosauroid

*Dilong paradoxus* (Xu et al., 2004), the oviraptorosaur *Incisivosaurus gauthieri* (Xu et al., 2002a), the ornithomimosaurs *Shenzhousaurus orientalis* (Ji et al., 2003) and *Hexing qingyi* (Jin et al., 2012), the dromaeosaurid *Graciliraptor lujiatunensis* (Xu & Wang, 2004a), and the troodontids *Sinovenator changii* (Xu et al., 2002b), *Mei long* (Xu & Norell, 2004), *Sinuronosus magnodens* (Xu & Wang, 2004b), *Daliansaurus liaoningensis* (Shen et al., 2017), and *Liaoningvenator curriei* (Shen et al., 2017). Among ornithischians, psittacosaurids are extremely abundant, being represented by the species *Psittacosaurus lujiatunensis* (including *P. major* and *Hongshanosaurus houi*; Hedrick & Dodson, 2013). The neoceratopsian *Liaoceratops yanzigouensis* (Xu et al., 2002a) and the ornithomimid *Jeholosaurus shangyuensis* (Xu et al., 2000) complete the dinosaur fauna.

Here we describe a new ornithischian dinosaur from the Lujiatun Beds, represented by two subcomplete and articulated specimens housed in the Paleontological Museum of Liaoning (PMOL) in Shenyang. Although it superficially resembles *Jeholosaurus*, represented by numerous specimens in the same deposits, the observed differences suggest that this new taxon occupies a more basal phylogenetic position at the base of the clade Ornithomimidae.

## Material and Methods

### Origin of the studied specimens:

As it is the case for most of the dinosaur specimens known from western Liaoning Province, the holotype and referred specimens of *Changmiania liaoningensis* were acquired by the PMOL from local farmers, according to whom the specimens were collected in the Lujiatun Beds close to Lujiatun Village. The specimens were only partially prepared when they were acquired by the PMOL. JMOD AD00114 was subsequently carefully prepared by the PMOL technical staff. Careful examination by the authors of the present paper and X-ray analyses did not reveal any trace of forgery besides the usual restorations, and the probability that the specimens are composite is accordingly low. The anatomy of the two specimens is fully concordant and clearly different from the *Jeholosaurus* specimens described from the same formation. Moreover, the morphological and phylogenetic information collected from the studied specimens is not discordant with our current understanding of basal ornithomimid anatomy and evolution. Based on our close examination of the blocks and our previously accumulated rich experience with Liaoning specimens, we can therefore confidently guarantee the authenticity of the specimens.

### Phylogenetic nomenclature:

For consistency purpose, we have tried to comply as far as possible with the phylogenetic nomenclature adopted by [Butler et al. \(2008\)](#) and [Boyd \(2015\)](#) in some of the most recent revisions of ornithischian phylogeny. We therefore use the following definitions of higher-level ornithischian taxa in the present paper:

- Cerapoda [Sereno, 1986](#): *Parasaurolophus walkeri*, *Triceratops horridus*, their most recent common ancestor and all descendants ([Butler et al., 2008](#));
- Clypeodonta [Norman, 2015](#): *Hypsilophodon foxii*, *Edmontosaurus regalis*, their most recent common ancestor, and all of its descendants ([Norman, 2015](#));
- Genasauria [Sereno, 1986](#): *Ankylosaurus magniventris*, *Stegosaurus stenops*, *Parasaurolophus walkeri*, *Triceratops horridus*, *Pachycephalosaurus wyomingensis*, their most recent common ancestor and all descendants ([Butler et al., 2008](#)).
- Heterodontosauridae [Romer, 1966](#): all ornithischians more closely related to *Heterodontosaurus tucki* than to *Parasaurolophus walkeri*, *Pachycephalosaurus wyomingensis*, *Triceratops horridus*, or *Ankylosaurus magniventris* ([Sereno, 2005](#));
- Iguanodontia [Dollo, 1888](#): all ornithopods more closely related to *Parasaurolophus walkeri* than to *Hypsilophodon foxii* or *Thescelosaurus neglectus* ([Sereno, 2005](#));
- Jeholosaurinae ([Han et al., 2012](#)): all ornithopods more closely related to *Jeholosaurus shangyuanensis*, than to *Changmiania liaoningensis*, *Ordromeus makelai*, *Nanosaurus agilis*, *Hypsilophodon foxii*, or *Thescelosaurus neglectus* (modified from [Han et al., 2012](#));
- Marginocephalia [Sereno, 1986](#): *Triceratops horridus*, *Pachycephalosaurus wyomingensis*, their most recent common ancestor and all descendants ([Butler et al., 2008](#));
- Neornithischia [Cooper, 1985](#): all genasaurians more closely related to *Parasaurolophus walkeri* than to *Ankylosaurus magniventris* or *Stegosaurus stenops* ([Butler et al., 2008](#));
- Ornithischia [Seeley, 1887](#): all dinosaurs more closely related to *Triceratops horridus* than to *Passer domesticus* or *Saltasaurus loricatus* ([Butler et al., 2008](#));
- Ornithopoda [Marsh, 1881](#): all genasaurians more closely related to *Parasaurolophus walkeri* than to *Triceratops horridus* ([Butler et al., 2008](#));
- Orodrominae [Brown et al., 2013](#): all ornithopods more closely related to *Orodromeus makelae* than to *Nanosaurus agilis* or *Thescelosaurus neglectus* (this study);
- Parksosaurinae [Buchholz, 2002](#): all clypeodonts more closely related to *Parksosaurus warreni* than to *Thescelosaurus neglectus* or *Parasaurolophus walkeri* ([Boyd, 2015](#), modified);
- Thescelosauridae ([Sternberg, 1937](#)): *Thescelosaurus neglectus*, *Orodromeus makelai*, their most

recent common ancestor, and all of its descendants ([Brown et al., 2013](#));

- Thescelosaurinae [Sternberg, 1937](#): all neornithischians more closely related to *Thescelosaurus neglectus* than to *Orodromeus makelai* or *Nanosaurus agilis* ([Boyd, 2015](#), modified);
- Thyreophora [Nopcsa 1915](#): all genasaurians more closely related to *Ankylosaurus magniventris* than to *Parasaurolophus walkeri*, *Triceratops horridus*, or *Pachycephalosaurus wyomingensis* ([Butler et al., 2008](#)).

# Phylogenetic analysis:

To assess its phylogenetic position within ornithischian dinosaurs, we included *Changmiania liaoningensis* in an extensively modified version of the character-taxon matrix published by [Dieudonné et al. \(2016\)](#). Besides *Changmiania liaoningensis*, we have integrated 14 taxa that were not included in [Dieudonné et al. \(2016\)](#) data-matrix: *Ankylosauria*, *Archaeoceratops oshimai*, *Chaoyangsaurus youngi*, *Goyocephale lattimorei*, *Homalocephale calathocercos*, *Isaberrysaura mollensis*, *Kulindadromeus zabaikalicus*, *Laquintasaura venezuelae*, *Liaoceratops yanzigouensis*, *Morrosaurus antarcticus*, *Stegosauria*, *Stenopelix valdensis*, *Thescelosaurus assiniboensis*, and *Wannanosaurus yansiensis*. In the present analysis, we have not coded the basal ornithopod *Oryctodromeus cubicularis*, from the middle Cretaceous Blackleaf Formation of southwestern Montana and the Wayan Formation of southeastern Idaho, USA ([Varricchio et al., 2007](#); [Krumenacker, 2010](#)), pending the formal description of the numerous partial skeletons from the Wayan Formation ([Krumenacker, 2010](#)). The final analysis consequently includes 61 taxonomic units and 263 characters ([Table S1](#) provides the character descriptions, [Table S2](#) contains the final data matrix, and [Table S3](#), the character support for selected nodes). *Herrerasaurus ischigualastensis* was used as outgroup. The analysis of the dataset was run TNT (Tree Analysis using New Technology, [Goloboff et al. 2008](#)); all the characters were equally weighted and regarded as non-additive. We performed a first round of 100 “New Technology” search analyses, with default parameter, and then explored the shortest tree islands found performing Tree Bisection Reconnection analyses saving all shortest tree found. Bremer nodal support was calculated in TNT saving all trees up to 10 steps longer than the most parsimonious results.

**Institutional abbreviations:** IVPP: Institute of Vertebrate Paleontology and Paleoanthropology, Beijing, China; NHM: Natural History Museum, London, U.K.; PMOL: Paleontological Museum of Liaoning, Shenyang, China

# **Nomenclatural acts:**

The electronic version of this article in Portable Document Format (PDF) will represent a published work according to the International Commission on Zoological Nomenclature (ICZN), and hence the new names contained in the electronic version are effectively published under that Code from the electronic edition alone. This published work and the nomenclatural acts it contains have been registered in ZooBank, the online registration system for the ICZN. The ZooBank LSIDs (Life Science Identifiers) can be resolved and the associated information viewed through any standard web browser by appending the LSID to the prefix <http://zoobank.org/>. The LSID for this publication is: Genus name: [urn:lsid:zoobank.org:act:AE88C0EE-9C4B-463B-B271-EB2868D7C81E](http://zoobank.org/urn:lsid:zoobank.org:act:AE88C0EE-9C4B-463B-B271-EB2868D7C81E), Species name: [urn:lsid:zoobank.org:act:0F980B4C-1EB3-4137-93FB-2C38008EE5E2](http://zoobank.org/urn:lsid:zoobank.org:act:0F980B4C-1EB3-4137-93FB-2C38008EE5E2), Publication LSID: [urn:lsid:zoobank.org:pub:9C5F2451-4E00-4919-9FE9-14E6629FCF64](http://zoobank.org/urn:lsid:zoobank.org:pub:9C5F2451-4E00-4919-9FE9-14E6629FCF64). The online version of this work is archived and available from the following digital repositories: PeerJ, PubMed Central and CLOCKSS.

## **Systematic Paleontology**

**Dinosauria** [Owen, 1842](#)

**Ornithischia** [Seeley, 1887](#)

**Neornithischia** [Cooper, 1985](#)

**Ornithopoda** [Marsh, 1881](#)

***Changmiania liaoningensis* nov. gen., nov. sp.**

**Etymology** – *Changmian*: eternal sleep, in Chinese Pinyin; *liaoningensis*: from Liaoning.

**Holotype** – JMOL AD00114, a sub-complete articulated skeleton ([Figs. 1A](#) and [1B](#))

**Referred specimen** – JMOL LFV022, another sub-complete skeleton, in dorsal view ([Fig. 1C](#)).

**Locality and Horizon** – Lujiatun, Shangyuan, Beipiao City, western Liaoning, China; Lujiatun Beds, lowest beds of Yixian Formation, Barremian, Lower Cretaceous.

**Diagnosis** (autapomorphies preceded by an asterisk): Fused premaxillae; \*nasal laterally expanded, overhanging the maxilla; long and straight posterior process of palpebral, nearly contacting the postorbital; \*rostrocaudally elongated frontals: maximum length to width ratio > 4; \*no sagittal crest on parietal; infratemporal fenestra triangular in lateral view, wider dorsally than ventrally; jugal process of postorbital rostrocaudally narrow along its whole height; \*rostral process of squamosal straight and

rostromedially elongated; \*prominent caudal boss at the dorsolateral corner of the squamosal; \*ventral border of angular distinctly concave; six cervical vertebrae; seven fused sacral vertebrae; \*neural spines of the sacral vertebrae completely fused together, forming a craniocaudally-elongated continuous bar; fused scapulocoracoid; \*scapular blade asymmetrically expanded both ventrally and dorsally; \*paired ilia symmetrically inclined dorsomedially, partially covering the sacrum in dorsal view; dorsal margin of ilium regularly convex along the whole length of the bone.

## Description

### Skull

**Premaxilla** – The maxillary process of the premaxilla is particularly robust, trapezoidal in shape, and inclined both caudodorsally and dorsolaterally (Figs. 2 and 5A). It forms the entire caudal margin of the external naris. It regularly expands rostromedially as it extends dorsally. Its caudal border contacts the maxilla and its straight dorsal border, the nasal. Its caudodorsal corner contacts the lacrimal, excluding the maxilla from the nasal, as also observed in *Heterodontosaurus* (Sereno, 2012), *Kulindadromeus* (Godefroit et al., 2014), and larger *Jeholosaurus* specimens (Barrett & Han, 2009). The much smaller nasal process forms the rostromedial border of the external naris; as also observed in *Jeholosaurus* (Barrett & Han, 2009), it only participates in the rostral third of the narial dorsal margin (Figs. 2 and 5A). This process rapidly tapers both mediolaterally and dorsoventrally as it extends dorsally, terminating in a fine point, so that the external naris is highly constricted in dorsal view, at the level of the contact between the paired premaxillae and nasals (Figs. 3 and 4). The rostral end of the nasal slightly overlaps the caudal end of the premaxilla. In dorsal view, the premaxillae are nearly completely fused together; only the distal end of their nasal process is not fused. Extensive fusion of the premaxillae has been reported in *Oryctodromeus* and *Zephyrosaurus* and has been interpreted as an adaptation to burrowing behavior (Varricchio et al., 2007). The rostral surface of the paired premaxillae is rugose (Fig. 5A), as also observed in *Hypsilophodon* (Galton 1974), *Zephyrosaurus* (Sues 1980), *Jeholosaurus* (Barrett & Han, 2009), and *Changchunsaurus* (Jin et al., 2010), and likely served for the attachment of a rhamphotheca. The rugosities slightly overhang the rostromedial corner of the external naris. They extend along the rostromedial surface of the main body of the premaxilla and potentially obscure the presence of premaxillary foramina. Above those rugosities the lateral surface of the premaxilla is convex and forms a shelf, so that the external naris is strongly inset from the lateral surface of the premaxilla (Fig. 5A). It contrasts with the concave lateral surface of the



premaxilla in *Jeholosaurus* (Barrett & Han, 2009) and *Changchunsaurus* (Jin et al., 2010). There is no distinct external narial fossa, as observed in some *Jeholosaurus* specimens (Barrett & Han, 2009). The lateroventral border of the premaxilla lies at about the same level as the ventral margin of the maxilla (Fig. 2), as also observed in *Zephyrosaurus* (Sues, 1980, fig. 16), *Orodromeus* (Scheetz, 1999), *Jeholosaurus* (Barrett & Han, 2009), *Changchunsaurus* (Jin et al., 2010), and *Haya* (Makovicky et al., 2011).

The number of premaxillary teeth cannot be precisely evaluated. They are robust, with a well-marked constriction between the root and the crown (Fig. 5A). The crowns are clearly separated from each other, as in other basal cerapodans, including *Hypsilophodon* (Galton, 1974), *Yinlong* (Xu et al., 2006), *Jeholosaurus* (Barrett & Han, 2009), and *Changchunsaurus* (Jin et al., 2010). The crowns have a subconical shape, with bulbous crown bases; they taper apically and are slightly recurved. They do not bear denticles and their enamel is perfectly smooth.

**Maxilla** – On the rostral third of the maxilla, the ascending process is high and hook-like (Figs. 2 and 5B); its concave caudal border forms the rostral margin of the antorbital fenestra, whereas its straight rostral border contacts the premaxilla. The apex of the ascending process contacts the lacrimal. A small circular fossa is set rostrally at the base of the ascending process, at the junction with the premaxilla (Figs. 2 and 5B). A similar fossa is present in *Hypsilophodon* (Galton, 1974; NHM R197), *Jeholosaurus* (Xu et al., 2000), *Changchunsaurus* (Jin et al., 2010), *Haya* (Makovicky et al., 2011), and *Orodromeus* (Scheetz, 2009), and was identified as a synapomorphy of Ornithopoda by Butler et al. (2008). The tooth-bearing ramus is rostrocaudally elongated and maintains an approximately even height along most of its length (Fig. 5B). The teeth are inset along a buccal emargination, which is dorsally limited by a horizontal ridge that extends rostrally from the ventral margin of the jugal (Figs. 5B and 5C). Rostrally, this ridge becomes progressively weaker expressed. The distance between the horizontal ridge and the ventral margin of the external antorbital fenestra is significantly lesser than in *Changchunsaurus*, reflecting the larger size of the external antorbital fenestra. Within the buccal emargination the lateral surface of the maxilla is concave dorsoventrally. A horizontal series of small nutrient foramina extend ventrally to the horizontal ridge (Fig. 5B). The dorsal portion of the medial lamina of the maxilla is visible within the antorbital fossa (Fig. 5B).

Fifteen maxillary teeth can be observed on the right maxilla of the holotype. A short edentulous diastema, equivalent to the mesiodistal length of 1 or 2 crowns, is present at the rostral end of the maxilla (Fig. 5B), as in *Changchunsaurus* (Jin et al., 2010). The size of the maxillary crowns progressively increases up to the mid-length of the maxilla. The crowns are poorly preserved and/or partly destroyed during preparation. The maxillary crowns overlap one another in an imbricate fashion: the distal part of each

crown laterally overlaps the mesial part of the succeeding crown (Fig. 5C). The crowns are low, with a mesiodistal length that is similar to their apicobasal height. Small denticles are present on the apical half of the crown and are generally supported by ridges that extend basally up to a weak basal cingulum; the ridges look better developed than in *Jeholosaurus* (Barrett & Han, 2009) and *Changchunsaurus* (Jin et al., 2010), more closely resembling the condition in *Hypsilophodon* (Galton, 1974). The maxillary crowns of *Orodromeus* apparently lack ridges supporting their marginal denticles (Scheetz, 1999). A low median eminence is usually developed on the labial, but a prominent primary ridge is absent.

**Lacrimal** – As is usual in basal cerapodans, the lacrimal consists of a ventral and dorsal process forming an inverted ‘L’ in lateral view (Figs. 2 and 6A). Both processes form an angle of approximately 120 degrees, as in *Jeholosaurus*. The dorsal portion of the ventral process is slightly longer rostrally than its ventral part. This process separates the rostral margin of the orbit from the caudal margin of the antorbital fossa; it contacts ventrally the maxilla and the jugal. The dorsal process extends rostrally to contact the maxillary process of the premaxilla. Its dorsal border contacts the prefrontal and nasal; ventrally it participates in the apical margin of the antorbital fossa and it contacts the ascending process of the maxilla (Fig. 6A).

**Nasal** – In dorsal view, the paired nasals taper rostrally above the external nares, where they contact the fused premaxillae to form the internarial bar; they quickly expand laterally and overhang the maxilla (Fig. 3). At this level, their lateral margin is particularly thickened. There is obviously no row of foramina along the lateral aspect of the nasal, as observed in *Jeholosaurus* (Xu et al., 2000; Barrett & Han, 2009). The caudolateral border of the nasal is notched by the contact facet for the prefrontal. Its caudal margin forms a concave articular surface for the frontal (Fig. 3). The dorsal surface of the paired nasals forms a deep longitudinal depression (Fig. 4), present in a number of basal neornithischians (Barrett et al., 2005), basal ornithomorphs, and ceratopsians, but which appears better developed than in other taxa in which this structure was described so far, including *Jeholosaurus* (Xu et al., 2000; Barrett & Han, 2009), *Haya* (Makovicky et al., 2011), *Liaoceratops* (Xu et al., 2002a), and *Yinlong* (Xu et al., 2006).

**Prefrontal** - the prefrontal is a strap-like element that participates in the rostradorsal margin of the orbit. It articulates with the lacrimal ventrally, the nasal medially and overlaps the frontal caudally (Figs. 3 and 4). Its straight lateral border forms an extended articulation surface with the palpebral. There is no ventral

process descending from the rostral end of the prefrontal, as observed in *Orodromeus* (Scheetz, 1999) and *Haya* (Makovicky et al., 2011).

**Supraorbital (palpebral)** - The rostral end of the palpebral forms a medial and a rostral process that both articulate with the lateral edge of the prefrontal. The caudal process of the palpebral is robust, perfectly straight and particularly, long, spanning over nearly the entire diameter of the orbit (Fig. 4). However, it likely did not articulate with the postorbital as in *Agilisaurus* (Peng 1992; Barrett et al. 2005). There is no trace of a postpalpebral, in articulation with the postorbital, as observed in *Thescelosaurus* (Boyd, 2014) and *Haya* (Makovicky et al., 2011). Together with the nasals and the prefrontals, the palpebrals formed a wide visor overhanging and likely protecting the antorbital and orbital regions of the skull.

**Frontal** – In dorsal view, the frontal is subrectangular and slightly convex rostrocaudally. It is particularly craniocaudally elongated, more than two times as long the parietal, and mediolaterally narrow: its maximum length to width ratio is  $> 4$  (Fig. 4). It therefore contrasts with the distinctly wider frontal in other basal ornithomichians, ornithomorphs, and ceratopsians: *Jeholosaurus* (3: Barrett & Han, 2009), *Agilisaurus* (3.0: Peng, 1992), *Hexinlusaurus* (2.2: He & Cai, 1984), *Hypsilophodon* (3.2: Galton, 1974), *Zephyrosaurus* (3.0: Sues, 1980), *Orodromeus* (2.2: Scheetz, 1999), *Thescelosaurus* (1.9, Galton, 1997), *Liaoceratops* (2.2: Xu et al., 2002a), *Psittacosaurus* (1.8 : Sereno et al., 1988), and *Yinlong* (1.8: Xu et al., 2006). Each frontal forms about three quarters of the dorsal margin of the orbit, and the orbital rim is thin and rugose, as is typical of basal ornithomorphs (Norman et al., 2004a; Makovicky et al., 2011); in *Jeholosaurus* (Barrett & Han, 2009), and *Haya* (Makovicky et al., 2011), the frontal comprises approximately 50% of the dorsal orbital margin. Rostrally, the paired frontals wedge between the nasals and are slightly overlapped by the prefrontals along their orbital margins. Caudolaterally, they form a straight contact with the postorbital and their caudal border is notched by the rostral process of the parietal. The frontals are excluded from the margin of the supratemporal fenestra by a direct contact between the postorbital and parietal (Figs. 3 and 4).

**Parietal** – The parietal is wide and robust, and its dorsal surface is regularly convex without any trace of a sagittal crest (Figs. 3 and 4), unlike in *Jeholosaurus* (Barrett & Han 2009), *Haya* (Makovicky et al., 2011), *Hypsilophodon* (Galton, 1974) and *Zephyrosaurus* (Sues, 1980). Rostrally, the parietals form a rounded process that wedge between the caudal margins of the frontals; in *Jeholosaurus*, on the contrary, the parietals are notched at the midline to receive a short triangular process from the caudal

margin of the frontals ([Barrett & Han, 2009](#)). Lateral to this point, the margin of the parietal produces a sinuous articulation with the frontals in dorsal view. The paired parietals are slightly constricted in dorsal view at the level of the middle part of the supratemporal fenestra. The rostromedial corner of the parietal flares laterally. The caudomedial corner of the parietal also extends laterally to contact the squamosal. The caudal border of the parietals forms a straight articulation with the supraoccipital. In *Jeholosaurus* ([Barrett & Han, 2009](#)) and *Haya* ([Makovicky et al., 2011](#)), the caudal edge of the parietal is deeply notched at the midline. There is no trace of a nuchal crest in *Changmiania*.

**Supraoccipital** – The surface of the supraoccipital is highly eroded. It is inserted between the lateral wings of the caudal end of the parietal and has a rhomboidal outline. It is steeply inclined rostromedially and. Its ventral border forms the dorsal rim of the foramen magnum.

**Postorbital** – In lateral view, the postorbital has the shape of an inverted ‘L’ and is formed by a jugal and a squamosal processes, meeting at an angle of about 90 degrees ([Fig. 2](#), [Fig. 6B](#)). Unlike other basal neoceratopsians, ornithomimids and ceratopsians, the postorbital is not rostromedially widened at the level of the junction between both processes, so that it does not look subtriangular in lateral view; consequently, the dorsal portion of the infratemporal fenestra is rostromedially wider than its ventral portion, so that the infratemporal fenestra is triangular in shape ([Figs. 2](#) and [6B](#)), contrasting with the elliptical infratemporal fenestra, with a dorsoventral long axis and a reduced dorsal margin, in other basal neoceratopsians, ornithomimids and ceratopsians described so far. The postorbital and infratemporal fenestra more closely resemble the condition in *Heterodontosaurus* ([Charig & Crompton, 1974](#)). The jugal process is straight, slightly inclined rostromedially, and, as already described, its rostromedial end remains equal along its whole height. It forms the dorsal half of the caudal margin of the orbit and rostral margin of the infratemporal fenestra; ventrally, it overlaps the dorsal process of the jugal. The squamosal process is quite short and tapers caudally ([Fig. 6B](#)); it is overlapped by the rostral process of the squamosal. In dorsal view, the postorbital forms a short medial process that contacts the frontal medially, and the parietal caudomedially. As in *Changchunsaurus*, there is no trace of rugosities on the lateral surface of the postorbital. Nodular ornamentation is present on the postorbital in *Jeholosaurus* ([Butler & Han, 2009](#)), and in some basal ceratopsians (e.g., *Archaeoceratops* (IVPP V11114) and *Yinlong* ([Xu et al., 2006](#))). In *Haya* ([Makovicky et al., 2011](#)), *Zephyrosaurus* ([Sues, 1980](#)) and *Orodromeus* ([Scheetz, 1999](#)), a rugose crest, which could have served as an area of attachment for the

postpalpebral, projects from the orbital rim near the juncture of the ventral and medial rami, (Makovicky et al., 2011).

**Squamosal** - The squamosal participates in the caudal and lateral margins of the supratemporal fenestra, and in the dorsocaudal margin of the infratemporal fenestra. The rostral process is particularly long and perfectly straight (Figs. 2 and 6B), as a consequence of the important rostrocaudal elongation of the dorsal margin of the infratemporal fenestra; it largely overlaps the squamosal process of the postorbital, reaching the postorbital process of the latter (Fig. 6B). The medial process is robust and triangular in dorsal view; its dorsal surface is inclined caudoventrally. The dorsolateral corner of the squamosal forms a prominent caudal boss, which forms the dorsocaudal corner of the skull in lateral view (Fig. 6B). The quadrate cotyle is cup-shaped; the pre- and postquadratic processes are not preserved.

**Quadrate** – The quadrate closely resembles that of *Changchunsaurus*. Its dorsal third is distinctly curved backwards in lateral view, so that its articulation with the squamosal is located caudal to the level of the quadrate condyles (Figs. 2 and 6C). The quadrate head is rounded in lateral view and is not offset from the shaft. The lateral wing of the quadrate is wide and concave rostrocaudally; its rostral border is sigmoidal in lateral view and participates in the caudodorsal margin of the infratemporal fenestra (Fig. 6C); ventrally, it is particularly thickened along its long contact area with the quadratojugal. Ventrally, the lateral condyle is partially exposed on the right quadrate; it is distinctly offset below the level of the maxillary tooth row, as observed in virtually all ornithischians, including basal forms such as *Lesothosaurus* (Norman et al., 2004b; Jin et al., 2010).

**Quadratojugal** – The quadratojugal is trapezoidal in lateral view and mediolaterally compressed (Figs. 2 and 6C); it participates in the caudoventral margin of the infratemporal fenestra. Its caudal portion extensively overlaps the rostroventral margin of the quadrate, but it does not reach the ventral process of the squamosal, unlike in *Heterodontosaurus* (Crompton & Charig, 1962), *Lesothosaurus* (Sereno, 1991), and the basal iguanodontians *Dryosaurus* and *Dysalotosaurus* (Norman, 2004). The rostral portion of the quadratojugal is overlapped by the caudal ramus of the jugal. As in *Changchunsaurus* (Jin et al., 2010), *Parksosaurus* (Galton, 1973), and some specimens of *Orodromeus* (Scheetz, 1999), there is no trace of a quadratojugal foramen; a circular foramen pierces the lateral surface of the quadratojugal in *Hypsilophodon* (Galton, 1974), *Jeholosaurus* (Xu et al., 2000), *Haya* (Makovicky et al., 2011), and

*Tenontosaurus* (Winkler et al., 1997). Caudoventrally, the quadratojugal extends above the quadrate condyles, as also observed in most basal cerapodans, including *Hypsilophodon* (Galton, 1974), *Jeholosaurus* (Barrett & Han, 2009), *Changchunsaurus* (Jin et al., 2010), *Haya* (Makovicky et al., 2011), *Orodromeus* (Scheetz, 1999), *Psittacosaurus* (Sereno et al., 1988), and *Yinlong* (Xu et al., 2006). In advanced ornithopods, the dorsoventral extent of the quadratojugal is reduced and the ventral margin does not approach the quadrate condyles (Norman, 2004).

**Jugal** - As in *Jeholosaurus* (Barrett & Han, 2009), *Changchunsaurus* (Jin et al. 2010), and basal neoceratopsians (You & Dodson, 2003; Xu et al., 2002a, 2006), the jugal is bowed outwards quite strongly along its length (Fig. 3). As in *Haya* (Makovicky et al., 2011), the lateral surface of the jugal lacks the ornamentation or jugal bosses seen in *Jeholosaurus* (Barrett & Han, 2009), *Changchunsaurus* (Jin et al., 2010), *Orodromeus* (Scheetz, 1999), and *Zephyrosaurus* (Sues, 1980). The rostral process of the jugal regularly tapers rostrally; it forms the ventral margin of the orbit and contacts the maxilla and the lacrimal (Fig. 6C). The dorsal process of the jugal is slightly inclined caudodorsally. It is laterally overlapped by the jugal process of the postorbital and participates in the ventral halves of the rostral margin of the infratemporal fenestra and of the caudal margin of the orbit. The caudal process is rather short, dorsoventrally high and mediolaterally compressed. It forms the ventral margin of the infratemporal fenestra. Its suture with the quadratojugal is rather complex: ventrally, it forms a long and slender projection extending below the ventral edge of the quadratojugal (Fig. 6C). There is no dorsocaudal projection, so that the caudal end of the jugal does not appear bifid as in *Jeholosaurus* (Barrett & Han, 2009), *Haya* (Makovicky et al., 2011), *Thescelosaurus* (Boyd, 2014), and possibly *Changchunsosaurus* (Jin et al., 2010).

## Lower jaw

**Predentary** – The predentary is partly eroded and only visible in right lateral view (Fig. 2). It is an elongate arrow-shaped element that tapers rostrally to a sharp, slightly upturned, point, as also observed in *Jeholosaurus* (Xu et al., 2000), *Changchunsaurus* (Jin et al., 2010), and *Archaeoceratops* (You & Dodson, 2003). A horizontal sulcus extends along the lateral margin of the predentary, separating the rostralateral and rostroventral processes. The caudoventral process is particularly elongated and slightly bowed rostroventrally, extending along the rostroventral border of the dentary.

**Dentary** – The dentary is elongated and rather robust, forming about 56% of the length of the mandible (Fig. 2). Its dorsal and ventral margins remain subparallel along most of their length. The rostral end of the dentary is not slightly downturned as in *Changchunsaurus* (Jin et al., 2010). The lateral side of the dentary is dorsoventrally convex; the tooth row is strongly inset and is separated from lateral side of the dentary by a well-developed buccal platform, limited ventrally by a low ridge. There is no trace of a rugose thickening of the rostrrodorsal margin of the dentary and of a horizontal groove extending ventral and adjacent to the tooth row, as observed in *Changchunsaurus* (Jin et al., 2010). The dorsoventral height and transverse width of the buccal emargination remain approximately constant along its length. Small foramina irregularly perforate the lateral surface of the dentary. The number of dentary teeth cannot be ascertained in the holotype, because they are obscured by the overlying maxillae; in any case, more than 15 teeth were present. An edentulous diastema was likely developed along the rostral portion of the dentary, as in *Changchunsaurus* (Jin et al., 2010). Caudally, the dentary contributes to the rostral half of a high and stout coronoid process that slopes caudodorsally. The relative position of the last dentary teeth relatively to the coronoid process cannot be observed. The caudal border of the dentary is dorsoventrally concave and overlaps the lateral surfaces of the angular and surangular. At mid-height, it forms a large triangular spur that extends caudally between the angular and surangular (Fig. 7). This spur is slightly developed in *Hypsilophodon* (Galton, 1974), *Jeholosaurus* (Barrett & Han, 2009), *Haya* (Makovicky et al., 2011), but is absent in *Changchunsaurus* (Jin et al., 2010) and *Thescelosaurus* (Boyd, 2014). The rostral end of the dentary terminates in a triangular process, limited dorsally and ventrally by facets for articulation with the prementary (Fig. 2). The dorsal facet, which articulates with the caudolateral process of the prementary, faces rostrally and slightly medially. The ventral facet, which articulates with the caudoventral process of the prementary, is much longer than the dorsal facet and faces ventrolaterally.

The dental teeth are present in their sockets, but they are obscured by the sediment or le overlying maxillary teeth. Therefore, they cannot adequately be described.

**Surangular** - The right surangular is partly exposed in lateral view, but a large portion is obscured by the jugal and quadratojugal (Figs. 2 and 7). The surangular forms the caudal half of the coronoid process. Its lateral margin forms a wide concave sulcus, close to the junction with the dentary and angular.

**Angular** - The angular is a rostrocaudally-elongated element that forms the posteroventral portion of the mandible (Figs. 2 and 7). It contacts the dentary rostrally and is overlapped dorsally by the



surangular. Its lateral surface is dorsoventrally convex. It forms a long caudoventral process that supports the articular and the ventral surface and participates in the ventral margin of the retroarticular process (Fig. 7). The rostral portion of the ventral border of the angular is straight, then it becomes distinctly concave, so that the caudoventral margin of the mandible looks notched in lateral view; this character seems autapomorphic for *Changmiania*.

**Articular** – The articular is relatively massive and is inserted between the angular ventrally and the surangular laterally. It forms a prominent retroarticular process that extends caudally over 1 cm beyond the caudal margin of the quadrate (Fig.7).

## Axial skeleton

The complete vertebral series is preserved and mostly articulated in the holotype specimen. Only the very tip of the tail is potentially missing. However, because the specimen lies on its belly, the vertebrae are still partly embedded within the matrix, and in most cases, only the neural arches and spines are visible. The important extension of ossified tendons along the dorsals and sacrals and the presence of articulated ribs still complicates the description of the vertebral series.

**Cervical vertebrae and ribs** - The neck of *Changmiania* is extremely shortened, formed by only 6 vertebrae. In basal ornithischians, ornithopods and ceratopsians, the neck is usually composed of nine vertebrae, as occurs in *Heterodontosaurus* (Santa Luca, 1980), *Hexinlusaurus* (He and Cai, 1984; Barrett et al., 2005), *Agilisaurus* (Peng, 1992), *Hypsilophodon* (Galton, 1974), *Jeholosaurus* (Han et al., 2012), *Changchunsaurus* (Butler et al., 2011), *Haya* (Makovicky et al., 2011), and *Orodromeus* (Scheetz, 1999). *Psittacosaurus* species possess 8 or 9 cervical vertebrae (Sereno, 1987), basal neoceratopsians usually 10 (You and Dodson, 2004), and iguanodontians also have more than 9 cervical vertebrae. In ornithischians, a reduced number of cervical vertebrae was only observed in the thyreophoran lineage so far, including the basal thyreophoran *Scelidosaurus* (six cervicals; Owen, 1863; Norman et al., 2004c), *Scutellosaurus* (six or seven cervicals; Norman et al., 2004c), and ankylosaurs (seven to eight cervicals; Vickaryous et al., 2004).

Cranially, a discrete atlantal intercentrum is tentatively identified on the left side of the specimen, although it is still nearly completely embedded in the matrix. The centrum of the axis appears longer than that of the succeeding cervical vertebrae (Fig. 8A). Its lateral surface is strongly concave



craniocaudally. The diapophysis is visible on the right lateral surface of the centrum, close to the suture with the neural arch. It means that the axial rib (not preserved in this specimen), was double-headed, as in *Agilisaurus* (Peng, 1992), *Jeholosaurus* (Han et al., 2012), *Haya* (Makovicky et al., 2011), *Orodromeus* (Scheetz 1999), and *Psittacosaurus*, contrasting with the single-headed axial ribs in *Hypsilophodon* (Galton, 1974) and *Changchunsaurus* (Butler et al., 2011). In lateral view, the neural spine is oriented posterodorsally at an angle of about 30 degrees to the horizontal. It is particularly elongate, extending well beyond the caudal border of the axial centrum to overlap cervical vertebra 3, as also observed in *Lesothosaurus* (Sereno, 1991), *Heterodontosaurus* (Santa Luca, 1980), *Jeholosaurus* (Han et al., 2012), *Changchunsaurus* (Butler et al., 2011), and *Haya* (Makovicky et al., 2011). Along its midline, the spine forms a particularly sharp crest extending along its entire length. The posterior margin of the axial neural spine is expanded transversely to form a frill-like plate above the cranial aspect of cervical 3. The postzygapophyses are set on the laterocaudal corner of the frill and face ventrally.

The longest cervical is cervical 3; there is apparently then a slight decrease in length until cervical 6, as also noticed in *Changchunsaurus* (Butler et al., 2011). The lateral surfaces of the centra are concave both anteroposteriorly and dorsoventrally. The neural arch of cervical 3 is much longer than its corresponding centrum, resembling a somewhat reduced version of the axial neural arch (Fig. 8A). Its caudal margin is also slightly expanded transversely, supporting robust ventrally-facing postzygapophyses. The neural arches become progressively shorter through cervicals 3–6. On the contrary, the diapophyses become progressively more robust and elongate. On cervical 4, the diapophyses projects caudoventrally, forming an angle of approximately 45° with the horizontal plane in lateral view (Fig. 8A); on cervicals 5 and 6, their orientation gradually changes from caudoventral to caudolateral. At their base, the prezygapophyses are prominent, facing dorsomedially. The neural spine is incipiently developed on cervical 3, as is usual in small ornithischians; it is distinctly better developed both in *Jeholosaurus* (Han et al., 2012) and *Changchunsaurus* (Butler et al., 2011). The neural spines gradually become more prominent and hook-like on cervicals 4–6 (Fig. 8B). The postzygapophyses remain large and robust, but progressively face more laterally.

Cervical ribs 4–6 are partially preserved and progressively increase in length. Rib 4 is clearly double-headed (Fig. 8B).

**Dorsal vertebrae and ribs** – All the dorsal vertebrae are concealed by matrix, and their dorsal surface is covered by a dense lattice of ossified tendons (Fig. 8B), so that their description is very limited. There are 15 or 16 dorsal vertebrae in *Changmiania*, as also reported in *Hypsilophodon* (Galton, 1974),

*Jeholosaurus* (Han et al., 2012), *Changchunsaurus* (Butler et al., 2011), and *Haya* (Makovicky et al., 2011); the dorsal series of heterodontosaurids and basal neoceratopsians appears shorter, with 13 dorsals reported in *Heterodontosaurus* (Sereno, 2012) and 12 in *Archaeoceratops* (You & Dodson, 2003). The transverse processes lie at the same level as the zygapophyses, as is usual in basal ornithopods (Norman et al., 2004a). At the cranial end of the dorsal series, the transverse processes are oriented dorsolaterally, but they rapidly shift to a more horizontal orientation further toward the sacrum. The neural spines are rather low; they are inclined caudally at the cranial end of the dorsal series, but progressively become more vertical further toward the sacrum. At the caudal end of the dorsal series, several neural spines appear fused together, although it can also be an artefact of preparation.

Dorsal ribs are rather robust; the longest lie along the level of dorsals 5-8 (Fig. 8B). The anterior dorsal ribs are dorsoventrally compressed, strongly curved, and are slightly grooved along their cranial and caudal surfaces. The last dorsal rib is notably short and robust and projects laterally; its distal extremity lies about the level of the cranial end of the preacetabular process of the ilium. It is apparently single-headed.

**Sacral vertebrae** – Only the neural spines of the sacral vertebrae are visible on the holotype specimen. They are completely fused together, forming a craniocaudally-elongated continuous bar (Fig. 8C), whose apex lies slightly dorsally to the level of the dorsal edge of the ilium. Such a complete fusion is unusual in small ornithischians, although it might also be explained by ontogeny. Consequently, the number of sacral vertebrae is tentatively estimated at 7. Six sacral vertebrae occur in many basal ornithischians, ornithopods, and ceratopsians, including *Heterodontosaurus* (Sereno, 2012), *Fruitadens* (Butler et al., 2012), some specimens of *Hypsilophodon* (Galton, 1974), *Jeholosaurus* (Han et al., 2012), *Haya* (Makovicky et al., 2011), *Orodromeus* (Scheetz, 1999), *Parksosaurus*, *Thescelosaurus* (Norman et al., 2004a), *Psittacosaurus* and *Archaeoceratops* (You and Dodson, 2003). Five sacral vertebrae are present in some basal ornithischians, including *Lesothosaurus* (Sereno, 1991), *Agilisaurus* (Peng, 1992), *Hexinlusaurus* (He and Cai, 1984; Barrett et al., 2005), probably *Eocursor* (Butler et al., 2007), and some specimens of *Hypsilophodon* (Galton, 1974). Sacra with more than six sacral vertebrae occur in *Oryctodromeus*, likely *Orodromeus* (Varricchio et al., 2007), derived iguanodontians (Norman, 2004) and ceratopsians (Dodson et al., 2004).

**Caudal vertebrae** – Thirty-six caudal vertebrae are preserved in the holotype specimen. Only few distalmost vertebrae are possibly missing. The tail is particularly long, making up to 55% of the total

length of the animal, and robust (Figs. 1A and 1C). The neural spines are developed along the 18 proximal vertebrae. Their height progressively decreases towards the distal end of the tail. More distally, the neural spine forms a low ridge along the dorsal surface of the neural arch. At all, the neural spines look more elongated proximodistally than in *Hypsilophodon* (Galton, 1974), and *Haya* (Makovicky et al., 2011).

The transverse processes of the proximal caudals are particularly prominent, tapering distally to a rounded terminus; they project horizontally and curve slightly posteriorly in their distal part (Fig. 8B). Passing through the caudal series, the transverse processes progressively become shorter, proportionally more massive, with a distal end that is slightly expanded proximodistally. The transverse processes completely disappear at about the level of the 20<sup>th</sup> caudal. The prezygapophyses extend proximally from the base of the neural arch to cover the postzygapophyses of the preceding vertebra, set at the ventrocaudal corner of the neural spine. The articular facets of the pre- and postzygapophyses are nearly vertical. The centrum of the distal caudal vertebrae becomes progressively more elongated proximodistally, becoming up to 4.5 times as long as high (Fig. 8C). Distal caudals remain proportionally shorter in *Jeholosaurus* (twice as long as high: Han et al., 2012). Both the pre- and postzygapophyses become very elongate, extending well beyond the proximal and distal limits of the centrum and exhibiting considerable overlap. The articular facets of the zygapophyses remain almost vertically inclined.

**Ossified tendons** - The ossified tendons form a particularly dense lattice alongside the neural spines of the dorsal and sacral vertebrae, extending cranially up to the dorsal surface of second dorsal vertebra (Figs. 8B and 8C). They are completely absent from the tail region. The tendons are relatively robust, and cylindrical in cross-section. They lack a distinct lattice-like arrangement and appear to be arranged in linear bundles. This distribution of ossified tendons is similar to that in the basal ornithischians *Lesothosaurus* (Thulborn, 1972), *Agilisaurus* (Peng, 1992), and *Heterodontosaurus* (Santa Luca, 1980), some basal ornithopods including *Jeholosaurus* (Han et al., 2012) and *Haya* (Makovicky et al., 2011). However, there is no evidence for the tendons extending onto anterior dorsals vertebrae in *Jeholosaurus* (Han et al., 2012). In *Hypsilophodon*, ossified tendons are also present alongside the dorsal and sacral regions, but they also extend up to the distal part of the tail (Galton, 1974). In *Psittacosaurus xinjiangensis*, ossified tendons extend on the proximal part of the tail (Sereno & Zhao, 1988). In the heterodontosaurid *Tianyulong*, few epaxial ossified tendons are present near the neural arches of the posterior dorsal, sacral and anterior caudal vertebrae, but a sheath of ossified tendons starts around the

seventh caudal vertebra, spanning the neural spines and chevrons and considerably stiffening the mid and distal portions of the tail (Sereno, 2012).

## Appendicular skeleton

**Scapula** - The scapula and the coracoid are fused together, forming an enlarged scapulocoracoid plate (Fig. 9). However, their respective limits of the bones can still be discerned. Among ornithopods, *Oryctodromeus* (Varricchio et al., 2007), *Koreanosaurus* (Huh et al., 2010), and *Haya* (Makovicky et al., 2011) possess fused scapulocoracoids. The scapula is slightly bowed medially and twisted along its length, following the outer contour of the rib cage. The proximal plate of the scapula is strongly expanded dorsoventrally. Its craniodorsal margin forms a strong deltoid ridge, which limits a vast deltoid fossa on the lateral side of the proximal plate (Fig. 8C). The acromial process projects craniodorsally to form a strong scapular spine, like in *Zephyrosaurus*, *Orodromeus* (Scheetz, 1999), *Oryctodromeus* (Varricchio et al., 2007), and *Koreanosaurus* (Huh et al., 2010). The scapula forms approximately 50% of the glenoid. Caudal to the glenoid, the cranioventral angle of the scapula forms a large buttress, which served as attachment site for a powerful *m. triceps scapularis lateralis externus* (Huh et al., 2010). Distal to the proximal plate, the scapular blade is also relatively robust (ratio length / minimal height of the scapula = 6.2). The distal end of the scapula is better preserved in the referred specimen JLUM LFV022 (Fig. 1C). As is usual in basal ornithopods, the ventral margin of the scapular blade is markedly concave in lateral view; however, the dorsal margin is also concave, although it remains nearly perfectly straight in e.g. *Hypsilophodon* (Galton, 1974), *Jeholosaurus* (Han et al., 2012), *Changchunsaurus* (Butler et al., 2011), *Haya* (Makovicky et al., 2011), *Zephyrosaurus*, *Orodromeus* (Scheetz 1999, fig.19), *Thescelosaurus* (Gilmore, 1915), and *Kulindadromeus* (Godefroit et al., 2014). Consequently, the distal end of the scapula is expanded both ventrally and dorsally in *Changmiania*, although the ventral expansion remains more important, contrasting with the more asymmetrical ventral expansion in other basal ornithopods. A strong posterior bend of the scapular blade is characteristic for *Oryctodromeus* (Varricchio et al. 2007).

**Coracoid** — The coracoid closely resembles that of *Hypsilophodon* (Galton 1974), *Orodromeus* (Scheetz 1999), and *Changchunsaurus* (Butler et al., 2011). In lateral view, it is subquadrate, with a convex cranial margin, and forms a robust cranioventral hook-like process (Fig. 9). Its ventral margin looks consequently notched. The coracoid forms about half of the glenoid; the glenoid surface of the coracoid is kidney-shaped. The coracoid is transversely expanded caudally at the level of the articular facet for

the scapula. The coracoid foramen is small, slit-like, and perforates the bone close to the articular facet for the scapula. The coracoid of *Changmiania* lacks a prominent cranioventrally extending ridge on its lateral surface, developed in *Psittacosaurus* (Averianov et al., 2006) and *Yandusaurus* (He and Cai 1984).

**Humerus** – The right humerus is visible in dorsal view and looks rather slender, contrasting with the much stouter humeri in *Oryctodromeus* and *Koreanosaurus*, in which the shafts are relatively shorter and wider relative to the total length of the bone (Varricchio et al., 2007; Huh et al., 2010). It is distinctly longer than the scapula (Table 1), as in *Kulindadromeus* (Godefroit et al., 2004), but unlike in *Jeholosaurus* (PG, pers. obs.) and *Haya* (Makovicky et al., 2011), in which the scapula and humerus are subequal in length. The proximal portion of the humerus is expanded transversely and compressed craniocaudally (Figs. 9A and 9B), with a regularly rounded proximal border. The humeral head forms a distinct thickening on the caudal surface, at the midpoint of the proximal border. The deltopectoral crest is obscured by the right coracoid but seems rather short, in any case proportionally shorter than in *Kulindadromeus* (Godefroit et al., 2014). The humeral shaft is slender and slightly compressed craniocaudally, with an elliptical cross-section. The distal end is slightly expanded laterally to form the two articular condyles. The lateral radial condyle and the medial ulnar condyle have similar sizes. The cranial surface of the distal end forms a shallow triangular depressed area (Figs. 9A and 9B).

**Ulna and radius** — The right ulna is completely preserved and visible in cranial view; the right radius is partly hidden by the ulna (Figs. 9A and 9B). The proximal portion of the left ulna is also visible in cranial view. The ulna and radius are distinctly shorter than the humerus (Table 1) and are rather robust. Both are nearly perfectly straight. The olecranon process of the ulna is moderately developed as is usual in basal ornithomorphs. On the proximal part of the ulna, the craniomedial coronoid process forms a low and rounded crest that progressively merges with the ulnar shaft. The craniolateral coronoid process is better developed and triangular in cranial view; its proximal portion overhangs the proximolateral side of the ulna. Between these processes, the articular facet for the proximal part of the radius is large, triangular and deeply concave. The ulna progressively tapers distally. Its distal end is slightly expanded mediolaterally again. Its cranial side forms a smoothly concave facet, slightly inclined laterally for the distal part of the radius. The right carpus and manus are eroded and partly hidden under the skull in the holotype JMOL AD00114 (Figs. 1A and 1B)

**Ilium** — The ilium of *Changmiania* closely resembles that of the basal neoceratopsian *Auroraceratops* (Morschhauser et al., 2019, fig. 21). Its dorsal margin is regularly convex along the whole length of the bone (Fig. 10A). It is straighter above the main plate and postacetabular process e.g. in *Kulindadromeus* (Godefroit et al., 2014), *Haya* (Makovicky et al., 2011), *Jeholosaurus* (Han et al., 2012), and *Thescelosaurus* (Gilmore, 1915). As also described in *Kulindadromeus* (Godefroit et al., 2014), the preacetabular process is about 40% of the ilium length, dorsoventrally narrow and strongly deflected ventrally, reaching the level of the pubic peduncle. As in *Jeholosaurus* (Han et al., 2012), *Haya* (Makovicky et al., 2011), *Hexinlusaurus* (He and Cai, 1984), and *Hypsilophodon* (Galton, 1974), the postacetabular process is slightly shorter, but dorsoventrally much higher than the preacetabular process, contrasting with the dorsoventrally narrow postacetabular process in *Kulindadromeus* (Godefroit et al., 2014). In *Orodromeus*, the postacetabular process is relatively longer than the preacetabular process (Scheetz, 1999), whereas the postacetabular process of *Heterodontosaurus* accounts for only ~25% of total ilium length (Santa Luca, 1980). There is no trace of a supraacetabular crest along its lateral surface. As in *Kulindadromeus* (Godefroit et al., 2014), *Haya* (Makovicky, 2011), and *Auroraceratops* (Morschhauser et al., 2019), the pubic peduncle is prominent, triangular in lateral view, and forms a 45° angle with the craniocaudal axis of the ilium body; the pubic peduncle is usually much reduced in most Cerapoda (Ösi et al., 2012). The ischiac peduncle projects ventrally and is stouter than the pubic peduncle. The acetabulum is deep and semi-circular, without any trace of a supraacetabular flange and of a medioventral acetabular flange. As in *Kulindadromeus* (Godefroit et al., 2014), *Jeholosaurus* (Han et al., 2012), *Changchunsaurus* (Butler et al., 2011), *Hypsilophodon* (Galton, 1974], and *Orodromeus* (Scheetz, 1999), the posterior portion of the brevis shelf cannot be observed in lateral view; it contrasts with the condition in basal ornithischians such as *Agilisaurus* (Peng, 1992), *Scelidosaurus*, *Lesothosaurus* (Butler, 2005), and *Haya* (Makovicky et al., 2011), in which the brevis fossa is visible in lateral view. In both the holotype and referred specimens of *Changmiania liaoningensis*, the paired ilia are not perfectly vertical, as it is the case in most ornithischians, but they are symmetrically inclined dorsomedially, partially covering the sacrum in dorsal view.

**Ischium** — Only the distal part of the paired ischial shafts is visible. They are dorsoventrally flattened and slightly expanded transversely, forming a distal ischial symphysis (Figs. 10B and 10C). Unfortunately, the precise extent of the distal symphysis cannot be accurately estimated in *Changmiania*. Elongate ischiac symphyses occur in *Agilisaurus* (Barrett et al., 2005), *Eocursor* (Butler, 2010), *Jeholosaurus* (Han et al., 2012), and likely in *Haya* (Makovicky et al., 2011). In *Agilisaurus*, the symphysis accounts for



approximately 50% of ischial length ([Barrett et al., 2005](#)), although the symphysis is much shorter in *Hypsilophodon* ([Galton, 1974](#)) and *Lesothosaurus* ([Butler, 2005](#)).

**Femur** — Both femora are visible in cranial, medial, and lateral view in both the holotype and referred specimens of *Changmiania liaoningensis*. Their proximal end is hidden under the ilia ([Figs. 1A-1C](#)). The femur of *Changmiania* is rather robust and slightly bowed dorsally ([Figs. 10B and 10C](#)). On the proximal portion of the femur, the lesser trochanter is eroded, but appears moderately developed and supported by a low ridge on the laterocranial corner of the proximal part of the femur; its apex lies well below the apex of the greater trochanter and the intertrochanteric cleft seems poorly developed. The cranial aspect of the femoral shaft is very convex. The distal end of the femur is slightly expanded laterally and compressed craniocaudally. The medial condyle is stouter than the lateral condyle. There is a shallowly concave triangular surface on the cranial side of the distal femur, but there is no real extensor intercondylar groove ([Figs. 10B and 10C](#)); this condition is also encountered in the basal ornithopods *Hypsilophodon* ([Galton, 1974](#): fig.54), *Orodromeus* ([Scheetz, 1999](#)), *Jeholosaurus* ([Han et al., 2012](#)), *Changchunsaurus* ([Butler et al., 2011](#)), and *Koreanosaurus* ([Huh et al., 2010](#)). This groove is much better developed in more derived ornithopods ([Butler et al. 2008](#)).

**Tibiotarsus** — Both tibiae are visible in dorsal view in both the holotype and referred specimens of *Changmiania liaoningensis* ([Figs. 1A-1C](#)); their proximal end is hidden by the overlapping femora. The astragalus and calcaneum are completely fused to the distal end of the tibia so their respective limits can be hardly discerned. The tibiotarsus is slender and about 120 % the length of the femur as in most basal ornithopods except *Koreanosaurus* (see [Table 2](#)). The caudal surface of the slender tibial shaft is regularly convex. Its distal end is flattened craniocaudally and slightly widened mediolaterally, with a shallowly concave caudal surface. The distal end of the tibiotarsus is regularly convex craniocaudally and concave mediolaterally. It is more salient distally at the level of the calcaneum and external malleolus of the tibia than at the level of the astragalus and internal malleolus of the tibia ([Figs. 10B and 10C](#)). The medial surface of the astragalus is flattened and inclined caudolaterally. The lateral surface of the calcaneum is depressed; its dorsal border is concave in lateral view, to fit the rounded distal end of the fibula.

**Fibula** — The fibula is rather robust ([Figs. 10B and 10C](#)). Its proximal end is craniocaudally expanded and transversely compressed. It regularly tapers distally, but its distal end is slightly expended transversely

again, with a rounded distal surface, to fit against the dorsal border of the calcaneum. The lateral side of the fibula is regularly convex craniocaudally, whereas its medial surface, which fits against the tibia, is deeply concave.

**Pes** - Both pedes are visible in cranial view (Figs. 10B-D). They are likely complete, but their medial part is covered by the tibiotasus and fibula. Left digit I is partly exposed. It is particularly short, extending up to the distal border of metatarsal II, and formed comprises two phalanges. In neither pes is it possible to ascertain the presence or absence of metatarsal 5. The pedal count is thus: 2-3-4-5-?. The metatarsals are tightly appressed to one another (Fig. 10D). Metatarsals II and IV are nearly equal in length and slightly shorter than metatarsal III. Metatarsal III and, especially, metatarsal IV curve laterally in cranial view. The distal articular condyles of the main metatarsals are shallowly developed on metatarsals II and IV, but metatarsal III has distinct lateral and medial condyles. The depression for attachment of the collateral ligaments is shallow on the medial surface of metatarsal II, whereas it is much more pronounced on both the medial and lateral sides of metatarsal III, and on the lateral side of metatarsal IV.

The phalanges of pes digits 2–4 have well-developed collateral ligament pits, dorsal extensor pits, and intercondylar processes (Figs. 10B-D). Their enlarged proximal articular surfaces are subdivided by a median ridge into two concavities. The ungual phalanges of digits 2 to 4 are elongate, exceeding the other phalanges in length, with deep lateral ligament grooves and sharp distal ends. The ungual of digit 3 is the longest (Fig. 10D), unlike in *Changchunsaurus*, in which the ungual of digit 2 slightly exceeds the ungual of digit 3 in length (Butler et al., 2011).

**Gastroliths** – A clustered mass of a dozen small pebbles is visible between the distal part of the right femur and the proximal part of the tibia in JMOL AD00114 (Fig. 1B). Individual clasts, which range in size from 5 mm to 13 mm, appear to be quartz or chert and are subangular in shape with a smooth patina (Fig. 10E). They closely resembles the pebble clusters associated to the holotype specimen of *Haya griva* (Makovicky et al., 2011).

## Phylogenetic analysis



Our phylogenetic analysis recovered 49 most parsimonious trees, with a length of 859 steps, a Consistency Index (CI) of 0.36 and a Retention Index (RI) of 0.62. The strict consensus of these trees is already well resolved, although the Bremer support remains low for most of the nodes (Fig. 11). This low support is mainly caused by various homoplasies (some of which are functionally significant), which are distributed widely across ornithischian phylogeny. A fully-resolved agreement subtree was obtained after the exclusion of 5 unstable ‘wildcard’ taxa (carried out using the ‘Comparisons-Agreement subtree(s)’ option of TNT; Fig. 12).

*Changmiania* is placed at the base of the clade Ornithopoda, characterized by the following unambiguous synapomorphies (Tables S2 and S3): rugosities are present on the rostral and dorsal surfaces of the premaxilla; there is a fossa-like depression on the premaxilla–maxilla boundary; the frontals are mediolaterally narrow and rostrocaudally elongate, at least twice as long as wide; in lateral view, the jugal extends ventrally above the distal condyles of the quadrate; and the olecranon process of the ulna is moderately developed.

However, *Changmiania* lacks the following synapomorphies, characteristic for more derived ornithopods grouped within the clade Thescelosauridae (Tables S2 and S3): the frontals are dorsally flattened over the orbit (they are still slightly arched in *Changmiania*); the rostral tip of the dentary is positioned at mid-height in lateral view (positioned above mid-height in *Changmiania*); the caudal neural spines extend beyond their own centrum (entirely positioned over the centrum in *Changmiania*); the scapula is longer or subequal to the humerus (the humerus is substantially longer than the scapula in *Changmiania*); and the ischiac peduncle of the ilium is broadly swollen and projects ventrolaterally (it is much reduced and projects ventrally in *Changmiania*).

*Jeholosaurus shangyuanensis*, also from the Lujiatun Beds of western Liaoning, is placed as a basal member of the thescelosaurid clade (Figs. 11 and 12). Together with *Haya griva* and *Changchunsaurus parvus*, it forms the clade Jeholosaurinae, characterized by the following synapomorphies (Tables S2 and S3): a forked caudal ramus of the jugal (dorsocaudal projection absent in *Changmiania*) and relatively wide coracoid ( $L/W < 0.6$ ;  $> 0.7$  in *Changmiania*).

Jeholosauridae form with more derived ornithopods a clade named Thescelosaurinae, characterized by the following synapomorphies (Tables S2 and S3): rod-like palpebrals (in *Changmiania*, the palpebrals have a much wider base); the presence of a quadratojugal foramen (absent in *Changmiania*), 6 fused vertebral centra (7 in *Changmiania*); the longest caudal transverse process is distal to the first caudal vertebra (at the level of the first caudal in *Changmiania*); and the proximal and distal edges of the cranioventral buttress form an acute, less than 75°, angle ( $> 75^\circ$  in *Changmiania*).

The present analysis recovers *Kulindadromeus zabaikalicus*, from the Middle Jurassic of Siberia ([Godefroit et al., 2014](#)), as the sister-taxon of Marginocephalia ([Figs. 11 and 12](#)), with whom it shares the following unambiguous synapomorphies: the shaft is strongly bowed laterally along its length in cranial and caudal views (it relatively straighter in *Changmiania*), and the pubic and iliac peduncles of the ischium are subequal in size, or the iliac peduncle is larger than the pubic peduncle (polariry unknown in *Changmiania*). Using the same dataset of the main analysis, we tested the alternative placement of *Kulindadromeus* as the sister-taxon of Cerapoda, as originally hypothesized by [Godefroit et al. \(2014\)](#); this analysis produced shortest trees that are two steps longer than the shortest trees resulted by the unconstrained analysis.

## Discussion

Vertebrate fossils unearthed from the lower Lujiatun Beds often retain a three-dimensional form, remaining perfectly articulated without any trace of weathering, scavenging or other disturbance ([Meng et al., 2004](#); [Zhao et al., 2007](#)). Moreover, some spectacular specimens from the Lujiatun Beds record exceptional behavioural information, such as evidence of parental care in the basal ceratopsian *Psittacosaurus* ([Meng et al. 2004](#); [Zhao et al., 2007](#)) and avian-like sleeping posture in the troodontid *Mei* ([Xu & Norell, 2004](#); [Gao et al., 2012](#)). ‘Sleeping’ *Mei* display a stereotypical sleeping or resting posture found in living bird: the tail curls forward and under the neck, both the hind and fore limbs lie folded beneath the body, and the neck and head curve back between the shoulder and folded elbow toward the hindlimb ([Xu & Norell, 2004](#); [Gao et al., 2012](#)). Although the three-dimensional position of both the *Changmiania liaoningensis* holotype and referred specimens is markedly different from the ‘sleeping’ *Mei long* specimens and from the stereotypical resting posture in living birds, they share some characteristic also suggesting a resting posture: their body sits on their symmetrically folded hindlimbs, their forelimbs are also symmetrically folded next to their body, with their elbows slightly displaced laterally relative to the trunk ([Xu & Norell, 2004](#); [Gao et al., 2012](#)). Moreover, the trunk and the head of JMOD AD00114 curve laterocaudally, so that its head rests on its right manus. The neck of *Mei long* was much longer and flexible, so that the head of the ‘sleeping’ specimens curves back between the shoulder and folded elbow toward the hindlimb ([Xu & Norell, 2004](#); [Gao et al., 2012](#)). The main difference between the *Changmiania* and *Mei* ‘sleeping’ specimens is the orientation of their tail: in *Mei*, it curls forward and under the neck, whereas it remains nearly perfectly straight, oriented

backward in both *Changmiania* individuals. It must be noted that the tail of *Changmiania* was likely a rather rigid structure, with limited lateral flexibility: the transverse processes of the proximal caudals are particularly elongated, massive and curved backward, while the pre- and postzygapophyses of the distal caudals are particularly elongate, extending well beyond the proximal and distal limits of the centrum and exhibiting considerable overlap. Curling its tail under its neck in a *Mei*-like style was therefore likely impossible for *Changmiania*.

Such a perfect preservation of the skeleton in a lifelike posture, as observed in both the holotype and referred specimens of *Changmiania liaoningensis* and also in countless fossils from the Lujiatun Beds, implies that the animals were rapidly entombed while they were still alive ([Meng et al. 2004](#); [Zhao et al., 2007](#)). Direct sedimentological investigation of the available *Changmiania* specimens is unfortunately impossible because they are already too heavily prepared, and we lack information about their discovery context. [Zhao et al. \(2007\)](#) showed that the sediments entombing a herd of juvenile *Psittacosaurus* skeletons from the Lujiatun Beds near Liu Tai village in western Liaoning represent a lahar (volcanic mudflow), either during the eruptive phase of a nearby volcanic center, or during a non-eruptive debris flow that reworked previously deposited volcanic material. This scenario might be extended to other exceptionally-preserved specimens from the same beds, but again we cruelly lack precise stratigraphic, sedimentological and taphonomic information about those specimens as most were discovered by local farmers and most of them were heavily restored. [Gao et al. \(2012\)](#) argued that lifelike posture of vertebrate fossils from the Lujiatun beds contradicts burial in a low energy lahar at least for those specimens: even a low energy lahar is likely to move a small animal out of a perimortem position.

It has also been proposed that some of the most fossiliferous locations in the Yixian Formation, and particularly in the Lujiatun Beds, are the result of instant catastrophic mass mortality events preserved in tuffaceous ashes ([Chang et al., 2008](#); [Gao et al., 2003](#); [Xu & Norell, 2004](#)); in such a Pompei-like scenario, the main cause of death for the vertebrates from the Lujiatun beds would have been asphyxiation by toxic volcanic gases of ashes. This hypothesis implies a brief but painful agony, which is certainly not supported by the apparent peaceful lifestyle posture of the *Mei* and *Changmiania* specimens. [Faux & Padian \(2007\)](#) suggest that death resulting from asphyxiation, toxins and infections can be reflected by an opisthotonic posture (hyperextension of the spine with both neck and tail recurved over the back) of the fossil skeleton; this posture is frequent in the two-dimensionally preserved specimens from the Jianshangou and Dawangzhangzi beds of the Yixian Formation, but is markedly different from the 'sleeping' dinosaurs from the Lujiatun Beds. However, [Reisdorf & Wuttke](#)

(2012) interpret the opithotonic posture as a post-mortem rather than a perimortem phenomenon, depending on the varying decay resistance of the soft tissues. Gao et al. (2012) similarly show that the troodontid specimens (and also the *Changmiania* fossils) from the Lujiatun Beds lack the ‘pugulistic’ hyperflexion of hands and toes often observed in humans that perished in pyroclastic flows and surges at Pompei and Herculaneum, interpreted as a perimortem response to death from high temperatures and fire (Mastolorenzo et al., 2010).

Meng et al. (2004) and Gao et al. (2012) propose that sudden entrapment in a collapsed underground burrow might be an alternative mechanism explaining the preservation of lifelike postures in small dinosaurs together with the complete absence of weathering and scavenging traces. Varricchio et al. (2007) first convincingly demonstrated that the basal ornithopod *Oryctodromeus* was probably a burrowing dinosaur: skeletal remains of an adult and two juveniles were found in the expanded distal chamber of a sediment-filled burrow and this dinosaur exhibits features of the snout, shoulder girdle and pelvis consistent with digging habits, while retaining cursorial hindlimb proportions. Although associated burrows are currently unknown for *Zephyrosaurus*, *Orodromeus*, and *Koreanosaurus*, the skeletal features shared by these basal ornithopods, together with sedimentological and taphonomic data, suggest that they might also been specialized for digging (Varricchio et al., 2007; Huh et al., 2010). The phylogenetic analysis presented here (Figs. 11 and 12) places *Zephyrosaurus*, *Orodromeus*, and *Koreanosaurus* in a monophyletic clade named Orodrominae. As already pointed out, *Oryctodromeus* has not been included in the present phylogenetic analysis, pending the formal description of the abundant material from Idaho (Krumenacker, 2010). However, previous analyses strongly suggest that *Oryctodromeus* is also an orodromine ornithopod (Varricchio et al., 2007; Boyd, 2015). Brown et al. (2013) also place *Albertadromeus syntarsus*, from the Oldman Fm of Alberta (Canada) amongst Orodrominae. However, this taxon is too fragmentary to be included in the present analysis.

*Changmiania* also displays a series of osteological features that are compatible with a fossorial behaviour in this basal ornithopod. Some extant fossorial vertebrates (e.g. the mole-rat *Spalax*) dig with their head to some degree, using the top of their broad, firm heads to move, loosen, or compact soil (Hildebrand, 1985). The fused premaxillae and the spatulate shape of the dorsal surface of the snout in *Changmiania* could represent such an implement. Among ornithopods, fused premaxillae are also present in the orodromine *Zephyrosaurus* and *Oryctodromeus* (Sues, 1980; Varricchio et al., 2007). However, nuchal crests are particularly developed in head-lifting diggers (Hildebrand, 1985), which is not the case in *Changmiania*.

The postcranial skeleton of *Changmiania* shares a series of morphological characteristics with actual scratch-digging mammals, including a shortened neck (6 cervical vertebrae), a radius that is significantly shorter (70%) than the humerus, and short hands ([Hildebrand 1985](#); [Elissamburu & De Santis, 2011](#)). Unfortunately, the ventral side of the ulna is hidden by sediments in both the holotype and referred specimens of *Changmiania*: in *Koreanosaurus* and *Orodromeus*, the proximal ulna is highly keeled as in Talpidae and in the anteater *Tamandua*, providing large insertion areas to both extensor and flexor muscles for the carpus and the digits, in relation with the digging function of the hands ([Lessertisseur & Saban, 1967](#); [Hildebrand, 1985](#); [Castiella et al., 1992](#); [Huh et al., 2010](#)). The enlarged, fused scapulocoracoid with prominent acromion and scapular spine, present in *Changmiania*, *Koreanosaurus* and *Oryctodromeus* would have increased attachment areas for muscles that were used to stabilize and operate digging forelimbs ([Hildebrand, 1985](#); [Varricchio et al. 2007](#); [Huh et al., 2010](#)).

The hip of *Changmiania* exhibits some features that might also tentatively be related to a digging behaviour. Actual mammals that dig with the forefeet usually brace with their hind feet, often supplemented by the tail serving as a prop ([Hildebrand, 1985](#)). Burrowing mammals such as the marsupial mole *Notoryctes* and, especially, Talpidae are able to keep their thighs relatively outspread from the axis of their body for a firmer bracing of the back of their body while digging; the pelvis of Talpidae is roughly horizontally oriented, nearly parallel with the vertebral column, and their acetabulum is consequently positioned higher, preventing torsion while bracing ([Lessertisseur and Saban, 1967](#)). In a similar way, the dorsomedial inclination of its paired ilia above its sacrum potentially helped *Changmiania* to keep its hindlimbs outspread and prevented torsion when digging.

The sacrum of *Changmiania* is long, formed by 7 co-ossified vertebrae as also observed in *Oryctodromeus*, likely *Orodromeus* ([Varricchio et al., 2007](#)), and larger Iguanodontia ([Norman, 2004](#)). Moreover, the neural spines of the sacral vertebrae are completely fused together in *Changmiania*, forming a craniocaudally-elongated continuous bar. Reinforcement of the sacropelvic complex, as observed in *Changmiania*, is also a distinctive feature of scratch-digging mammals and appear to relate to the forces, well in excess of body weight, that converge on the pelvic girdle during bracing with the hind feet ([Hildebrand, 1985](#)). The pelvis of *Zephyrosaurus*, *Oryctodromeus* and *Orodromeus* is further reinforced by a direct pubosacral contact, but this region is hidden by sediment in both available *Changmiania* specimens. As is frequently observed in burrowers ([Hildebrand, 1985](#); [Varricchio et al., 2007](#)), the basal portion of the tail is particularly robust in *Changmiania*, with elongated transverse processes and a high neural spine on the proximal caudal vertebrae.

The hindlimb of *Changmiania* is about twice as long as its forelimb and its tibia is significantly longer than its femur, as in most other small basal ornithopods except *Koreanosaurus* (Table 2); those hindlimb proportions suggest that *Changmiania* basically remained an efficient cursorial dinosaur. Moreover, the forelimb and skull modifications remain rather modest, so that *Changmiania* was obviously not a true subterranean animal, but more likely a facultative digger, as also suggested for *Oryctodromeus* (Varricchio et al., 2007).

A fossorial behavior in *Changmiania* therefore supports the hypothesis that both JMOL AD00114 and JMOL LfV022 were suddenly entrapped in a collapsed underground burrow, which would explain their perfect lifelike postures and the complete absence of weathering and scavenging traces, as proposed by Meng et al. (2004) and Gao et al. (2012). Of course, this hypothesis remains fully compatible with the observation that the sediments from the Lujiatun Beds mostly represent a lahar (Zhao et al., 2007). It can be hypothesized that the burrows containing the *Changmiania* carcasses collapsed during the debris flow episode; we can alternatively imagine that the *Changmiania* specimens dug they burrow in unstable reworked volcanic material just after the debris flow. Those explanations of course remain pure speculations, as firsthand stratigraphic and taphonomic data are lacking for the currently known *Changmiania* specimens.

# References

- Averianov AO, Voronkevich AV, Leshchinskiy SV, Fayngertz AV. 2006. A ceratopsian dinosaur *Psittacosaurus sibiricus* from the Early Cretaceous of West Siberia, Russia and its phylogenetic relationships. *Journal of Systematic Paleontology* 4(4):359–395.
- Barrett PM, Butler RJ, Knoll F. 2005. Small-bodied ornithischian dinosaurs from the Middle Jurassic of Sichuan, China. *Journal of Vertebrate Paleontology* 25:823–834 DOI 10.1671/0272-4634(2005)025[0823:SODFTM]2.0.CO;2.
- Barrett PM, Han F-L. 2009. Cranial anatomy of *Jeholosaurus shangyuanensis* (Dinosauria: Ornithischia) from the Early Cretaceous of China. *Zootaxa* 2072:31–55.
- Boyd CA. 2014. The cranial anatomy of the neornithischian dinosaur *Thescelosaurus neglectus*. *PeerJ* 2:3669 DOI 10.7717/peerj.669.
- Boyd CA. 2015. The systematic relationships and biogeographic history of ornithischian dinosaurs. *PeerJ* 3:e1523 DOI 10.7717/peerj.1523.
- Brown CM, Evans DC, Ryan MJ, Russell AP. 2013. New data on the diversity and abundance of small-bodied ornithopods (Dinosauria, Ornithischia) from the Belly River Group (Campanian) of Alberta. *Journal of Vertebrate Paleontology* 33:495–520 DOI 10.1080/02724634.2013.746229.



- 907 **Buchholz PW. 2002.** Phylogeny and biogeography of basal Ornithischia. In: Brown D E, ed. *The*  
908 *Mesozoic in Wyoming*. Casper: Tate Geological Museum, 18–34.
- 909 **Butler RJ. 2005.** The ‘fabrosaurid’ ornithischian dinosaurs of the Upper Elliot Formation (Lower  
910 Jurassic) of South Africa and Lesotho. *Zoological Journal of the Linnean Society* **145**:175–218 DOI  
911 [10.1111/j.1096-3642.2005.00182.x](https://doi.org/10.1111/j.1096-3642.2005.00182.x).
- 912 **Butler RJ. 2010.** The anatomy of the basal ornithischian dinosaur *Eocursor parvus* from the lower Elliot  
913 Formation (Late Triassic) of South Africa. *Zoological Journal of the Linnean Society* **160**:648–684  
914 DOI [10.1111/j.1096-3642.2009.00631.x](https://doi.org/10.1111/j.1096-3642.2009.00631.x).
- 915 **Butler RJ, Jin LY, Chen J, Godefroit P. 2011.** The postcranial osteology and phylogenetic position of  
916 the small ornithischian dinosaur *Changchunsaurus parvus* from the Quantou Formation (Cretaceous:  
917 Aptian-Cenomanian) of Jilin Province, northeastern China. *Palaeontology* **54**:667–683 DOI  
918 [10.1111/j.1475-4983.2011.01046.x](https://doi.org/10.1111/j.1475-4983.2011.01046.x).
- 919 **Butler RJ, Smith RMH, Norman DB. 2007.** A primitive ornithischian dinosaur from the Late Triassic  
920 of South Africa, and the early evolution and diversification of Ornithischia. *Proceedings of the Royal*  
921 *Society B* **274**:2041–2046 DOI [10.1098/rspb.2007.0367](https://doi.org/10.1098/rspb.2007.0367).
- 922 **Butler RJ, Upchurch P, Norman DB. 2008.** The phylogeny of the ornithischian dinosaurs. *Journal of*  
923 *Systematic Paleontology* **6**:1–40 DOI [10.1017/S1477201907002271](https://doi.org/10.1017/S1477201907002271).
- 924 **Castiella MJ, Laville E, Renous S, Gasc J-P. 1992.** Caractéristiques morphologiques du membre  
925 antérieur de la taupe commune, *Talpa europaea* (Mammalia, Talpidae). *Mammalia* **56**(2):265-285.
- 926 **Chang MM, Chen PJ, Wang YQ, Miao DS, editors. 2008.** *The Jehol fossils: the emergence of*  
927 *feathered dinosaurs, beaked birds and flowering plants*. New York: Academic Press, 208 pp.
- 928 **Charig AJ, Crompton AW. 1974.** The alleged synonymy of *Lycorhinus* and *Heterodontosaurus*.  
929 *Annals of the South African Museum* **64**:167–189.
- 930 **Cooper MR. 1985.** A revision of the ornithischian dinosaur *Kangnasaurus coetzeei* Haughton with a  
931 classification of the Ornithischia. *Annals of the South African Museum* **95**:281–317.
- 932 **Crompton AW, Charig AJ. 1962.** A new ornithischian from the Upper Triassic of South Africa. *Nature*  
933 **196**:1074–1077 DOI [10.1038/1961074a0](https://doi.org/10.1038/1961074a0).
- 934 **Dieudonné P-E, Tortosa T, Torcida Fernández-Baldor F, Canudo JI, Díaz-Martínez I. 2016.** An  
935 unexpected early rhabdodontid from Europe (Lower Cretaceous of Salas de los Infantes, Burgos  
936 Province, Spain) and a re-examination of basal iguanodontian relationships. *PLoS ONE*  
937 **11**(6):e0156251 DOI [10.1371/journal.pone.0156251](https://doi.org/10.1371/journal.pone.0156251).
- 938 **Dodson P, Forster CA, Sampson SD. 2004.** Ceratopsidae. In: Weishampel DB, Dodson P, Osmólska H,  
939 eds. *The Dinosauria*. Second edition. Berkeley: University of California Press, 494-513.
- 940 **Dollo L. 1888.** Iguanodontidae et Camptonotidae. *Comptes Rendus de l'Académie des Sciences (Paris)*  
941 **106**:775–777.
- 942 **Elissamburu A, De Santis L. 2011.** Forelimb proportions and fossorial adaptations in the scratch-  
943 digging rodent *Ctenomys* (Caviomorpha). *Journal of Mammalogy* **92**(3):683-689 DOI [10.1644/09-](https://doi.org/10.1644/09-MAMM-A-113.1)  
944 [MAMM-A-113.1](https://doi.org/10.1644/09-MAMM-A-113.1).

- 945 **Faux CM, Padian K. 2007.** The opisthotonic posture of vertebrate skeletons: postmortem contraction or  
946 death throes? *Paleobiology* **33**:201–226.
- 947 **Gao C, Morschhauser EM, Varricchio DJ, Liu J, Zhao B. 2012.** A second soundly sleeping dragon:  
948 new anatomical details of the Chinese troodontid *Mei long* with implications for phylogeny and  
949 taphonomy. *PLoS ONE* **7**(9):e45203 DOI [10.1371/journal.pone.0045203](https://doi.org/10.1371/journal.pone.0045203).
- 950 **Galton PM. 1973.** Redescription of the skull and mandible of *Parksosaurus* from the Late Cretaceous  
951 with comments on the family Hypsilophodontidae (Ornithischia). *Life Science Contributions, Royal*  
952 *Ontario Museum* **89**:1–21.
- 953 **Galton PM. 1974a.** The ornithischian dinosaur *Hypsilophodon* from the Wealden of the Isle of Wight.  
954 *Bulletin of the British Museum (Natural History) Geology* **25**:1–152.
- 955 **Galton PM. 1997.** Cranial anatomy of the basal hypsilophodontid dinosaur *Thescelosaurus neglectus*  
956 Gilmore (Ornithischia: Ornithopoda) from the Upper Cretaceous of North America. *Revue de*  
957 *Paléobiologie* **16**:231–258.
- 958 **Gilmore CW. 1915.** Osteology of *Thescelosaurus*, an orthopodous dinosaur from the Lance Formation of  
959 Wyoming. *Proceedings of the United States National Museum* **49**:591–616 DOI  
960 [10.5479/si.00963801.49-2127.591](https://doi.org/10.5479/si.00963801.49-2127.591).
- 961 **Godefroit P, Sinitsa SM, Dhouailly D, Bolosky YL, Sizov AV, McNamara ME, Benton MJ, Spagna**  
962 **P. 2014.** A Jurassic ornithischian dinosaur from Siberia with both feathers and scales. *Science*  
963 **345**:451–455 DOI [10.1126/science.1253351](https://doi.org/10.1126/science.1253351).
- 964 **Goloboff PA, Farris JS, Nixon KC. 2008.** TNT, a free program for phylogenetic analysis. *Cladistics*  
965 **24**:774–786 DOI [10.1111/j.1096-0031.2008.00217.x](https://doi.org/10.1111/j.1096-0031.2008.00217.x).
- 966 **Han F-L, Barrett PM, Butler RJ, Xing X. 2012.** Postcranial anatomy of *Jeholosaurus shangyuanensis*  
967 (Dinosauria, Ornithischia) from the Lower Cretaceous Yixian Formation of China. *Journal of*  
968 *Vertebrate Paleontology* **32**:1370–1395 DOI [10.1080/02724634.2012.694385](https://doi.org/10.1080/02724634.2012.694385).
- 969 **He HY, Wang XL, Zhou ZH, Jin F, Wang F, Yang LK, Ding X, Boven A, Zhu RX. 2006.** <sup>40</sup>Ar/<sup>39</sup>Ar  
970 dating of Lujiatun Bed (Jehol Group) in Liaoning, northeastern China. *Geophysical Research Letters*  
971 **33**:L04303 DOI [10.1029/2005GL025274](https://doi.org/10.1029/2005GL025274).
- 972 **He XL, Cai KJ. 1984.** *The Middle Jurassic dinosaurian fauna from Dashanpu, Zigong, Sichuan*. Vol. 1.  
973 Chengdu, Sichuan Scientific and Technological Publishing House 1–71.
- 974 **Hildebrand M. 1985.** Digging in quadrupeds. In: Hildebrand M, Bramble, DM, Liem KF, Wake DB,  
975 eds. *Functional vertebrate morphology*. Cambridge, MA: Belknap Press, 89–109.
- 976 **Hu Y, Meng J, Wang Y, Li C. 2005.** Large Mesozoic mammals fed on young dinosaurs. *Nature*  
977 **433**:149–152. DOI [10.1038/nature03102](https://doi.org/10.1038/nature03102).
- 978 **Huh M, Lee D-G, Kim J-K, Lim J-D, Godefroit P. 2011.** A new basal ornithopod dinosaur from the  
979 Upper Cretaceous of South Korea. *Neues Jahrbuch für Geologie und Paläontologie Abhandlungen*  
980 **259**:1–24 DOI [10.1127/0077-7749/2010/0102](https://doi.org/10.1127/0077-7749/2010/0102).
- 981 **Ji Q, Norrell M, Makovicky PJ, Gao K, Ji S, Yuan C. 2003.** An early ostrich dinosaur and implications  
982 for ornithomimosaur phylogeny. *American Museum Novitates* **3420**:1–19 DOI: [10.1206/0003-](https://doi.org/10.1206/0003-0082(2003)420<0001:AEODAI>2.0.CO;2)  
983 [0082\(2003\)420<0001:AEODAI>2.0.CO;2](https://doi.org/10.1206/0003-0082(2003)420<0001:AEODAI>2.0.CO;2)



- 984 **Jin LY, Chen J, Godefroit P. 2012.** A new basal ornithomimosaur (Dinosauria: Theropoda) from the  
985 Early Cretaceous Yixian Formation, Northeast China. In Godefroit P, ed. *Bernissart Dinosaurs and*  
986 *Early Cretaceous Terrestrial Ecosystems*. Bloomington and Indianapolis: Indiana University  
987 Press, 467–487
- 988 **Jin LY, Chen J, Zan SQ, Butler RJ, Godefroit P. 2010.** Cranial anatomy of the small ornithischian  
989 dinosaur *Changchunsaurus parvus* from the Quantou Formation (Cretaceous: Aptian-Cenomanian)  
990 of Jilin Province, northeastern China. *Journal of Vertebrate Paleontology* **30**:196–214 DOI  
991 [10.1080/02724630903409279](https://doi.org/10.1080/02724630903409279).
- 992 **Krumenacker LJ. 2010.** *Chronostratigraphy and paleontology of the mid-Cretaceous Wayan Formation*  
993 *of eastern Idaho, with a description of the first Oryctodromeus specimens from Idaho*. Provo:  
994 Department of Geological Sciences, Brigham Young University, 88 pp.
- 995 **Lessertisseur J, Saban R. 1967.** Squelette appendiculaire. In: Grassé P-P, éd. *Traité de Zoologie,*  
996 *tome 16 (1): Mammifères – tégument – squelette*. Paris: Masson, 707-1078.
- 997 **Makovicky PJ, Kilbourne BM, Sadleir RW, Norell MA. 2011.** A new basal ornithopod (Dinosauria,  
998 Ornithischia) from the Late Cretaceous of Mongolia. *Journal of Vertebrate Paleontology* **31**:626–  
999 640 DOI [10.1080/02724634.2011.557114](https://doi.org/10.1080/02724634.2011.557114).
- 1000 **Marsh OC. 1881.** Principal characters of American Jurassic dinosaurs. Part V. *American Journal of*  
1001 *Science, Series 3* **21**:417–423.
- 1002 **Mastolorenzo G, Petrone P, Pappalardo L, Guarino FM. 2010.** Lethal thermal impact at periphery of  
1003 pyroclastic surges: evidences at Pompeii. *PLoS ONE* **5**(6): e11127 DOI  
1004 [10.1371/journal.pone.0011127](https://doi.org/10.1371/journal.pone.0011127).
- 1005 **Meng Q, Liu J, Varricchio DJ, Huang T, Gao C. 2004.** Parental care in an ornithischian dinosaur.  
1006 *Nature* **431**: 145–146 DOI [10.1038/431145a](https://doi.org/10.1038/431145a).
- 1007 **Morschhauser EM, You H, Li D, Dodson P. 2019.** Postcranial morphology of the basal neoceratopsian  
1008 (Ornithischia: Ceratopsia) *Auroraceratops rugosus* from the Early Cretaceous (Aptian–Albian) of  
1009 northwestern Gansu Province, China". *Journal of Vertebrate Paleontology*. **38** (sup 1.): 75–116. DOI  
1010 [10.1080/02724634.2018.1524383](https://doi.org/10.1080/02724634.2018.1524383).
- 1011 **Nopcsa F. 1915.** Die Dinosaurier der siebenbürgischen Landesteile. *Mitteilungen aus dem Jahrbuche der*  
1012 *Königlich-Ungarischen Geologischen Reichsanstalt* **23**:1–26.
- 1013 **Norman DB. 2004.** Basal Iguanodontia. In: Weishampel DB, Dodson P, Osmólska H, eds. *The*  
1014 *Dinosauria*. Second edition. Berkeley: University of California Press, 413–437.
- 1015 **Norman DG. 2015.** On the history, osteology, and systematic position of the Wealden (Hastings group)  
1016 dinosaur *Hypselospinus fittoni* (Iguanodontia: Styracosterna). *Zoological Journal of the Linnean*  
1017 *Society* **173**:92–189 DOI [10.1111/zoj.12193](https://doi.org/10.1111/zoj.12193).
- 1018 **Norman DB, Sues H-D, Witmer LM, Coria RA. 2004a.** Basal Ornithopoda. In: Weishampel DB,  
1019 Dodson P, Osmólska H, eds. *The Dinosauria*. Second edition. Berkeley: University of California  
1020 Press, 393–412.

- 1021 **Norman DB, Witmer LM, Weishampel DB. 2004b.** Basal Ornithischia. In: Weishampel DB, Dodson P,  
1022 Osmólska H, eds. *The Dinosauria*. Second edition. Berkeley: University of California Press, 325–  
1023 334.
- 1024 **Norman DB, Witmer LM, Weishampel DB. 2004c.** Basal Thyreophora. In: Weishampel DB, Dodson  
1025 P, Osmólska H, eds. *The Dinosauria*. Second edition. Berkeley: University of California Press, 335–  
1026 342.
- 1027 **Ósi A, Prondvai E, Butler R, Weishampel DB. 2012.** Phylogeny, histology and inferred body size  
1028 evolution in a new rhabdodontid dinosaur from the Late Cretaceous of Hungary. *PLoS ONE*  
1029 **7(9):e44318** DOI [10.1371/journal.pone.0044318](https://doi.org/10.1371/journal.pone.0044318).
- 1030 **Owen R. 1842.** Report on British fossil reptiles, part II. *Report of the British Association for the*  
1031 *Advancement of Science for 1841* **9**:60–204.
- 1032 **Owen, R. 1863.** A monograph of the Fossil Reptilia of the Liassic Formations. Part II. A monograph of a  
1033 fossil dinosaur (*Scelidosaurus harrisonii* Owen) of the Lower Lias. *Palaeontographical Society*  
1034 *Monographs* **13**:1-26
- 1035 **Peng G. 1992.** Jurassic ornithopod *Agilisaurus louderbacki* (Ornithopoda: Fabrosauridae) from Zigong,  
1036 Sichuan, China. *Vertebrata Palasiatica* **30**:39–51.
- 1037 **Reisdorf AG, Wuttke M. 2012.** Re-evaluating Moodie’s oposthotonic–posture hypothesis in fossil  
1038 vertebrates Part I: Reptiles - the taphonomy of the bipedal dinosaurs *Compsognathus longipes* and  
1039 *Juravenator starki* from the Solnhofen Archipelago (Jurassic, Germany). *Palaeobiodiversity and*  
1040 *Palaeoenvironments* **92(1)**:119-168 DOI [10.1007/s12549-011-0068-y](https://doi.org/10.1007/s12549-011-0068-y).
- 1041 **Romer AS. 1966.** *Vertebrate paleontology*. 3rd edition. Chicago: University of Chicago Press, 468 pp.
- 1042 **Santa Luca AP. 1980.** The postcranial skeleton of *Heterodontosaurus tucki* (Reptilia, Ornithischia) from  
1043 the Stormberg of South Africa. *Annals of the South African Museum* **79**:159–211.
- 1044 **Scheetz RD. 1999.** *Osteology of Orodromeus makelai and the phylogeny of basal ornithopod dinosaurs*.  
1045 Bozeman: Montana State University, 186 pp.
- 1046 **Seeley HG. 1887.** On the classification of the fossil animals commonly named Dinosauria. *Proceedings*  
1047 *of the Royal Society of London* **43**:165–171 DOI [10.1098/rspl.1887.0117](https://doi.org/10.1098/rspl.1887.0117).
- 1048 **Sereno PC. 1986.** Phylogeny of the bird-hipped dinosaurs. *National Geographic Research* **2**:234–256.
- 1049 **Sereno PC. 1991.** *Lesothosaurus*, “fabrosaurids”, and the early evolution of Ornithischia. *Journal of*  
1050 *Vertebrate Paleontology* **11**:168–197 DOI [10.1080/02724634.1991.10011386](https://doi.org/10.1080/02724634.1991.10011386).
- 1051 **Sereno PC. 2005.** The logical basis of phylogenetic taxonomy. *Systematic Biology* **54**:595–619 DOI  
1052 [10.1080/106351591007453](https://doi.org/10.1080/106351591007453).
- 1053 **Sereno PC. 2012.** Taxonomy, morphology, masticatory function and phylogeny of heterodontosaurid  
1054 dinosaurs. *Zookeys* **226**:1–225 DOI [10.3897/zookeys.226.2840](https://doi.org/10.3897/zookeys.226.2840).
- 1055 **Sereno P, Zhao X. 1988.** *Psittacosaurus xinjiangensis* (Ornithischia: Ceratopsia), a new psittacosaur  
1056 from the Lower Cretaceous of northwestern China. *Journal of Vertebrate Paleontology* **8**:353–365.

- 1057 **Sereno, PC, Zhao X, Chang Z, Rao C. 1988.** *Psittacosaurus meileyingensis* (Ornithischia: Ceratopsia),  
1058 a new psittacosaur from the Lower Cretaceous of northeastern China. *Journal of Vertebrate*  
1059 *Paleontology* **8**:366–377.
- 1060 **Shen C, Lü J, Kundrát M, Brusatte SL, Gao H. 2017a.** A new troodontid dinosaur from the Lower  
1061 Cretaceous Yixian Formation of Liaoning Province, China. *Acta Geologica Sinica* **91(3)**:763–780  
1062 DOI [10.1111/1755-6724.13307](https://doi.org/10.1111/1755-6724.13307).
- 1063 **Shen C, Zhao B, Gao CL, Lü JC, Kundrát M. 2017b.** A new troodontid dinosaur (*Liaoningvenator*  
1064 *curriei* gen. et sp. nov.) from the Early Cretaceous Yixian Formation in western Liaoning province.  
1065 *Acta Geoscientica Sinica* **38(3)**:359–371.
- 1066 **Sternberg CM. 1937.** A classification of *Thescelosaurus*, with a description of a new species.  
1067 *Proceedings of the Geological Society of America* **1936**:375.
- 1068 **Sues H-D. 1980.** Anatomy and relationships of a new hypsilophodontid dinosaur from the Lower  
1069 Cretaceous of North America. *Palaeontographica Abteilung a Palaeozoologie-Stratigraphie* **169**:51–  
1070 72.
- 1071 **Thulborn RA. 1972.** The postcranial skeleton of the Triassic ornithischian dinosaur *Fabrosaurus*  
1072 *australis*. *Palaeontology* **15**:29–60.
- 1073 **Varricchio DJ, Martin AJ, Katsura Y. 2007.** First trace and body evidence of a burrowing, denning  
1074 dinosaur. *Proceedings of the Royal Society B: Biological Sciences* **274**:1361–1368 DOI  
1075 [10.1098/rspb.2006.0443](https://doi.org/10.1098/rspb.2006.0443).
- 1076 **Vickarious MK, Maryńska T, Weishampel DB. 2004.** Ankylosauria. In: Weishampel DB, Dodson P,  
1077 Osmólska H, eds. *The Dinosauria*. Second edition. Berkeley: University of California Press, 363–  
1078 392.
- 1079 **Winkler DA, Murry PA, Jacobs LL. 1997.** A new species of *Tenontosaurus* (Dinosauria:  
1080 Ornithopoda) from the Early Cretaceous of Texas. *Journal of Vertebrate Paleontology*  
1081 **17**:330–348 DOI [10.1080/02724634.1997.10010978](https://doi.org/10.1080/02724634.1997.10010978).
- 1082 **Xu X, Forster CA, Clark JM, Mo J. 2006.** A basal ceratopsian with transitional features from the Late  
1083 Jurassic of northwestern China. *Proceedings of the Royal Society B* **273**:2135–2140 DOI  
1084 [10.1098/rspb.2006.3566](https://doi.org/10.1098/rspb.2006.3566).
- 1085 **Xu X, Makovicky PJ, Wang XL, Norell MA, You HL. 2002a.** A ceratopsian dinosaur from China and  
1086 the early evolution of Ceratopsia. *Nature* **416**:314–317  
1087 DOI [10.1038/416314a](https://doi.org/10.1038/416314a).
- 1088 **Xu X, Norell MA, Wang XL, Makovicky PJ, Wu X-C. 2002b.** A basal troodontid from the Early  
1089 Cretaceous of China. *Nature* **415(6873)**:780–784 DOI [10.1038/415780a](https://doi.org/10.1038/415780a).
- 1090 **Xu X, Norell MA. 2004.** A new troodontid dinosaur from China with avian-like sleeping posture.  
1091 *Nature* **431(7010)**:838–841 DOI [10.1038/nature02898](https://doi.org/10.1038/nature02898).
- 1092 **Xu X, Wang X. 2004b.** A new dromaeosaur (Dinosauria: Theropoda) from the Early Cretaceous Yixian  
1093 Formation of Western Liaoning. *Vertebrata Palasiatica* **42(2)**:111–119.

1094 **Xu X, Wang X. 2004b.** A new troodontid (Theropoda: Troodontidae) from the Lower Cretaceous Yixian  
1095 Formation of Western Liaoning, China. *Acta Geologica Sinica—English Edition* **78(1)**:22–26 DOI  
1096 [10.1111/j.1755-6724.2004.tb00671.x](https://doi.org/10.1111/j.1755-6724.2004.tb00671.x).

1097 **Xu X, Wang XL, You HL. 2000.** A primitive ornithopod from the Early Cretaceous Yixian Formation of  
1098 Liaoning. *Vertebrata Palasiatica* **38**:318–325.

1099 **You HL, Dodson P. 2003.** Redescription of neoceratopsian dinosaur *Archaeoceratops* and  
1100 earl evolution of Neoceratopsia. *Acta Palaeontologica Polonica* **48**:261–272.

1101 **Zhao Q, Barrett PM, Eberth DA. 2007.** Social behavior and mass mortality in the basal ceratopsian  
1102 dinosaur Psittacosaurus (Early Cretaceous, People’s Republic of China). *Palaeontology* **50**:1023–  
1103 1029 DOI [10.1111/j.1475-4983.2007.00709.x](https://doi.org/10.1111/j.1475-4983.2007.00709.x).

1104

1105

# Figure Captions

**Figure 1** *Changmiania liaoningensis*, an ornithomimid dinosaur from the Lower Cretaceous of Lujiatun (Liaoning Province, China). (A) holotype JMW AD00114 in dorsal view; (B) anterior part of the holotype JMW AD00114 in caudolateral view; (C) referred specimen JMW LFV022 in dorsal view.

**Figure 2** Skull of JMW AD00114 in right lateral view. (A) photograph; (B) line drawing.

**Figure 3** Skull of JMW AD00114 in left dorsolateral view. (A) photograph; (B) line drawing.

**Figure 4** Skull of JMW AD00114 in dorsal view. (A) photograph; (B) line drawing.

**Figure 5** Skull of JMW AD00114 in right lateral view. (A) close-up of the premaxillary region; (B) close-up of the maxillary region; (C) close-up of the maxillary teeth.

**Figure 6** Skull of JMW AD00114. (A) antorbital fenestra region in right lateral view; (B) left squamosal and postorbital in dorsolateral view; (C) caudal half of the skull in right lateral view.

**Figure 7** Postdentary bones of JMW AD00114 in right lateral view.

**Figure 8** Axial skeleton of JMW AD00114. (A) cervical vertebrae 2 to 4 in right lateral view; (B) cervical and dorsal series in left lateral view; (C) sacrum and proximal caudal vertebrae in dorsal view; (D) distal caudal vertebrae in left lateral view. Abbreviations: ca: caudal vertebra; cv: cervical vertebra; d: dorsal vertebra.

**Figure 9** Right scapular girdle and forelimb of JMW AD00114. (A) photograph; (B) line drawing; (C) detail of the right scapulocoracoid in lateral view.

**Figure 10** Pelvic girdle and hindlimbs of JMW AD00114. (A) right ilium in lateral view; (B) photograph of distal ischia and right hindlimb; (C) line drawing of distal ischia and right hindlimb; (D) left foot in cranial view; (E) gastroliths.

**Figure 11** Phylogenetic position of *Changmiania liaoningensis* gen. et sp. nov. among Ornithischia. Strict consensus tree of 49 MPT's. Tree Length = 859. Nodal support (Bremer indices > 1) is indicated above or below the branches.

**Figure 12** Phylogenetic position of *Changmiania liaoningensis* gen. et sp. nov. among Ornithischia. Fully-resolved agreement subtree obtained after the exclusion of 5 unstable 'wildcard' taxa, carried out using the 'Comparisons-Agreement subtree(s)' option of TNT (Goloboff et al., 2008).

**Table 1.** Selected measurements of *Changmiania liaoningensis* JMW AD00114 specimen.

**Table 2.** Comparisons of postcranial measurements (in mm) in selected basal ornithomimids: *Changmiania liaoningensis*, *Koreanosaurus boseongensis*, *Hypsilophodon foxii*, *Orodromeus makelai*, and *Oryctodromeus cubicularis*.

# Figure 1

*Changmiania liaoningensis*, an ornithomimid dinosaur from the Lower Cretaceous of Lujiatun (Liaoning Province, China).

(A) holotype JMOD AD00114 in dorsal view; (B) anterior part of the holotype JMOD AD00114 in caudolateral view; (C) referred specimen JMOD LFV022 in dorsal view.



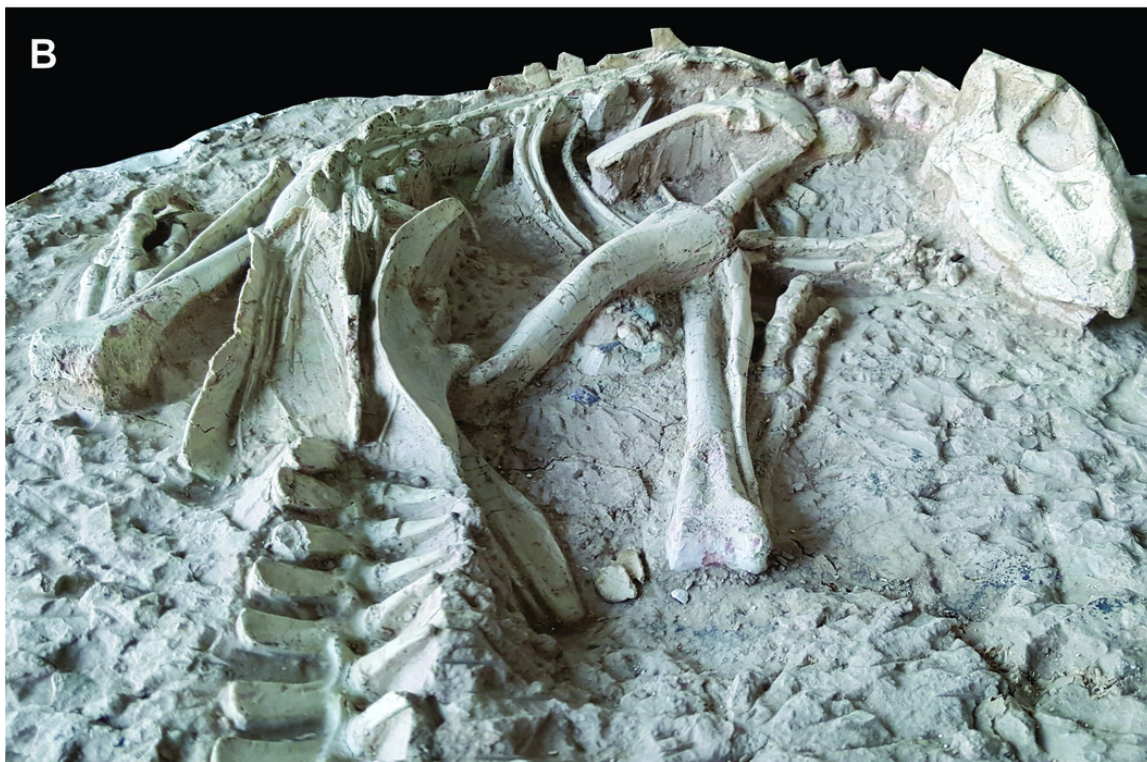
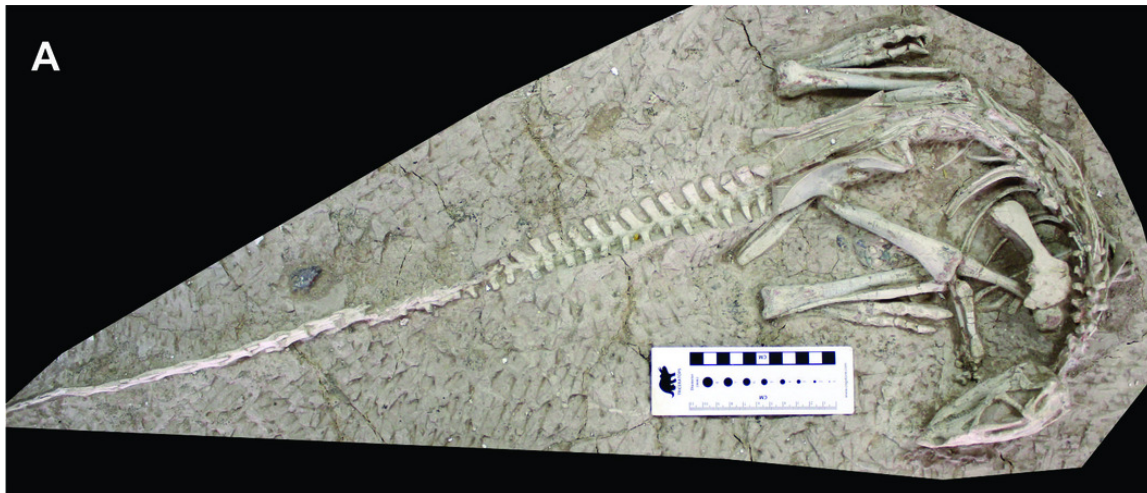


# Figure 2

Skull of JMOL AD00114 in right lateral view.

(A) photograph; (B) line drawing.



**A**



2 cm

**B**

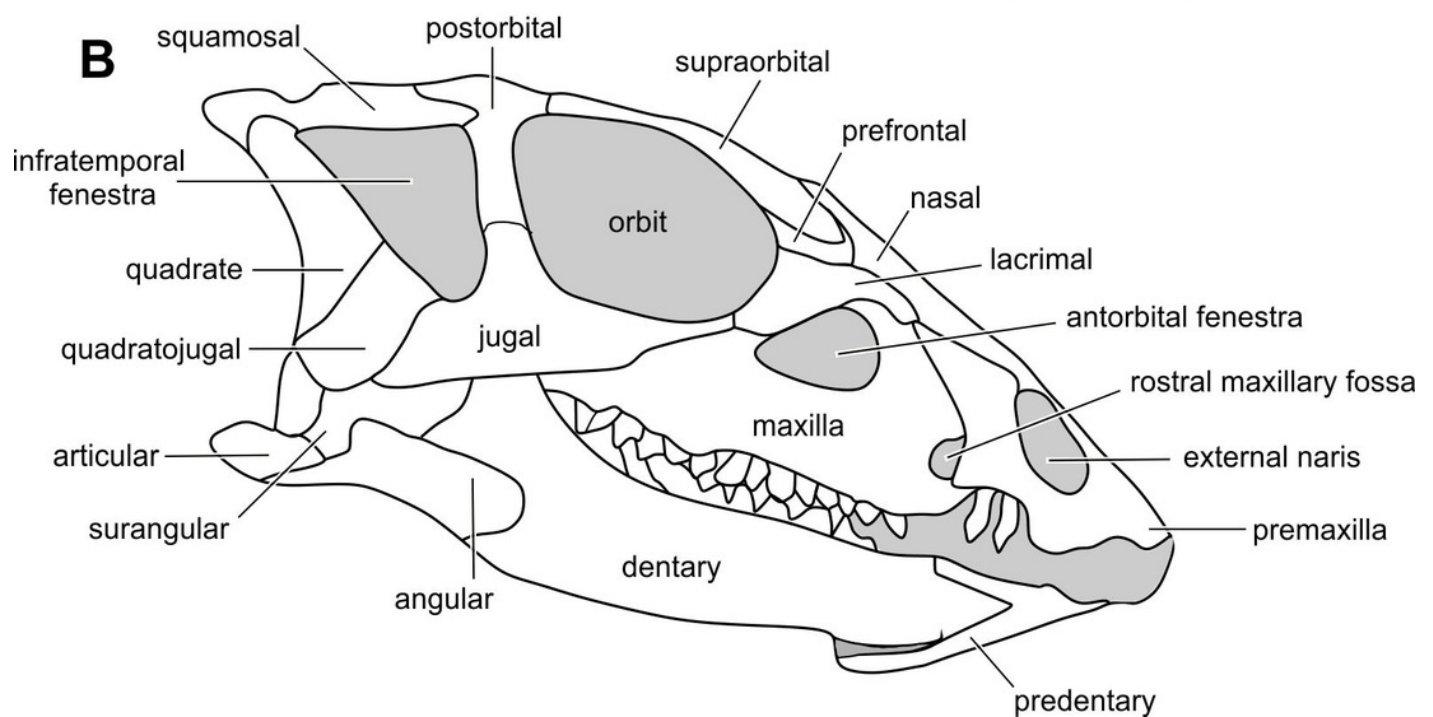


# Figure 3

Skull of JMOL AD00114 in left dorsolateral view.

(A) photograph; (B) line drawing.

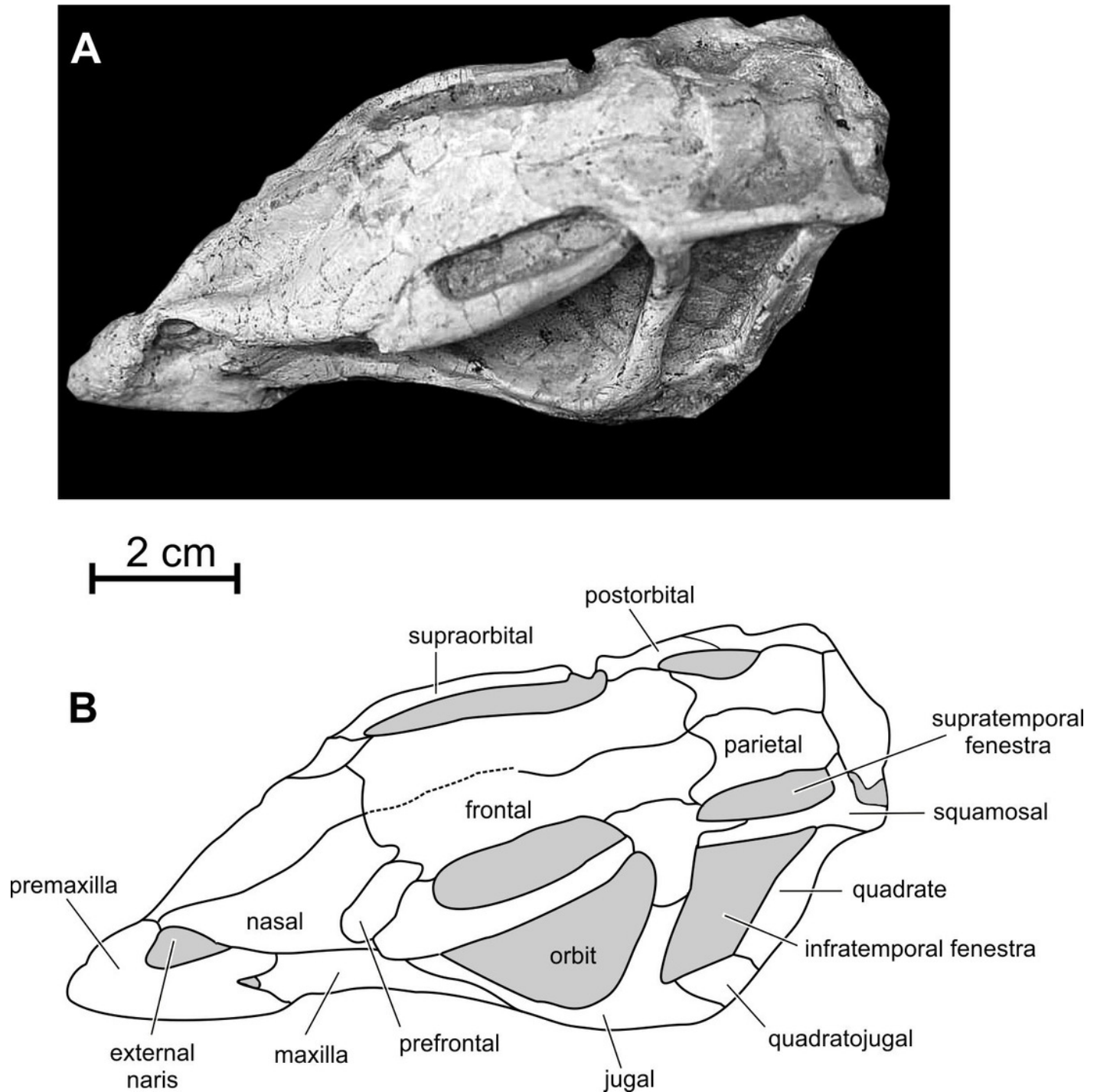


# Figure 4

Skull of JMOL AD00114 in dorsal view.

(A) photograph; (B) line drawing.

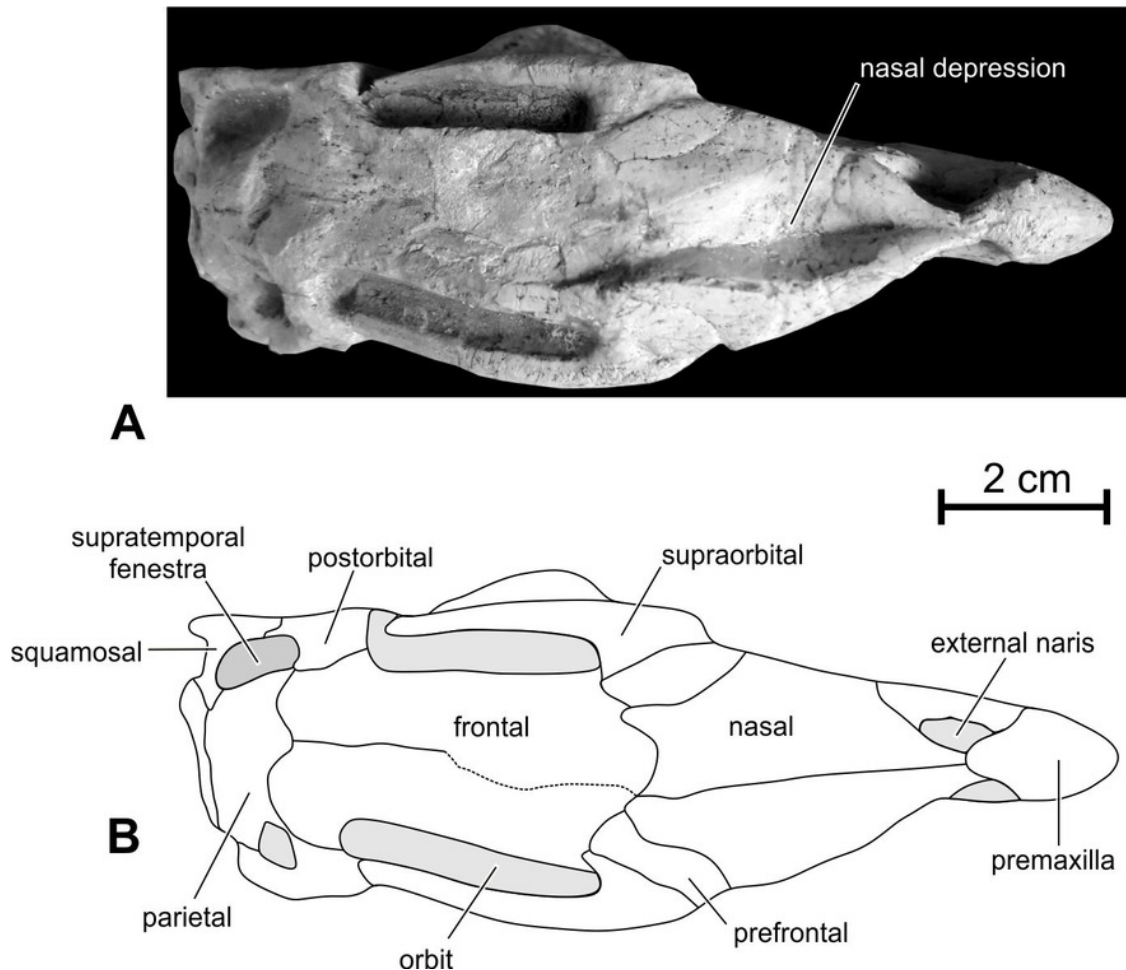


# Figure 5

Skull of JMOL AD00114 in right lateral view.

(A) close-up of the premaxillary region; (B) close-up of the maxillary region; (C) close-up of the maxillary teeth.



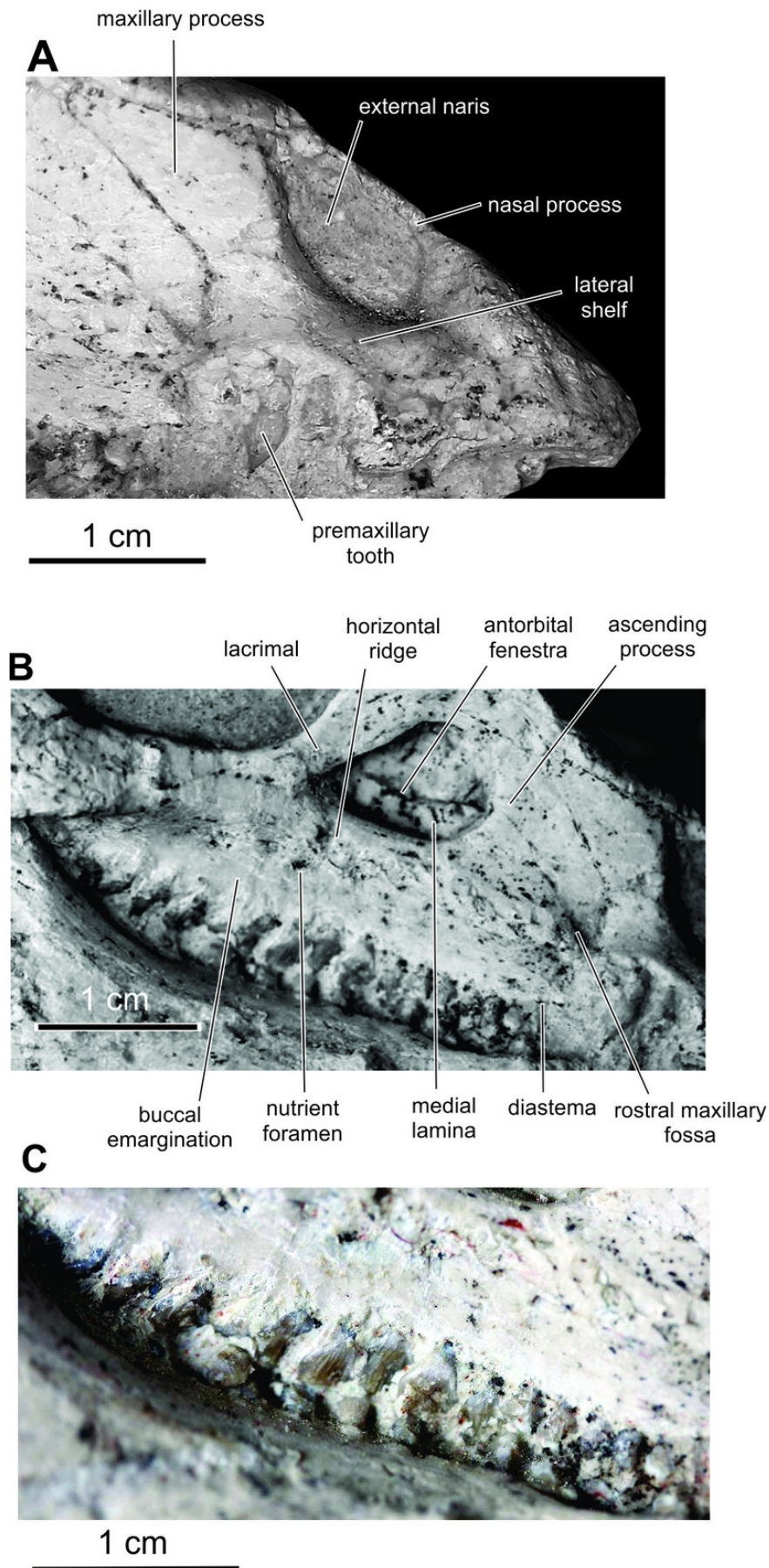


# Figure 6

Skull of JMOL AD00114.

(A) antorbital fenestra region in right lateral view; (B) left squamosal and postorbital in dorsolateral view; (C) caudal half of the skull in right lateral view.

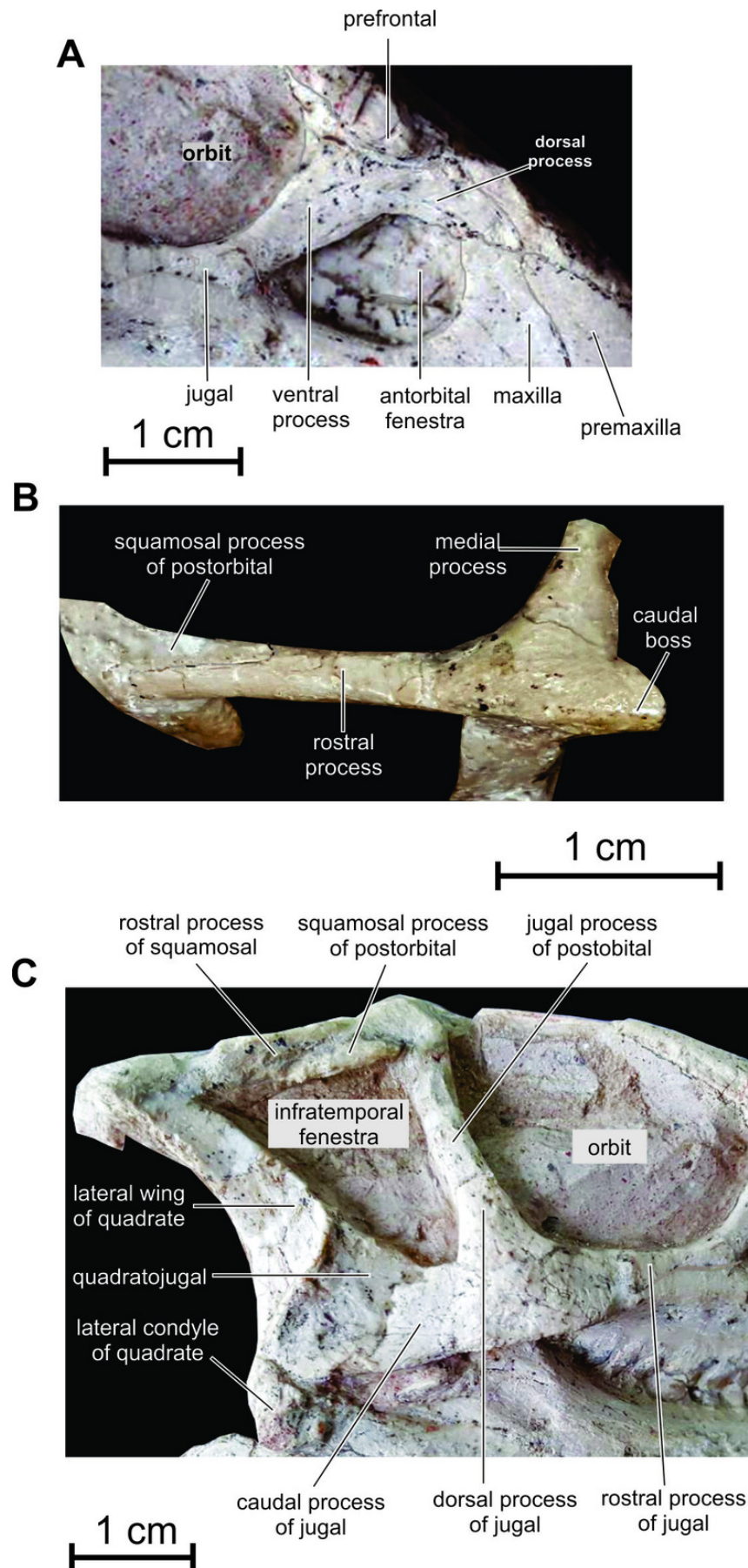




# Figure 7

Postdentary bones of JMOL AD00114 in right lateral view.

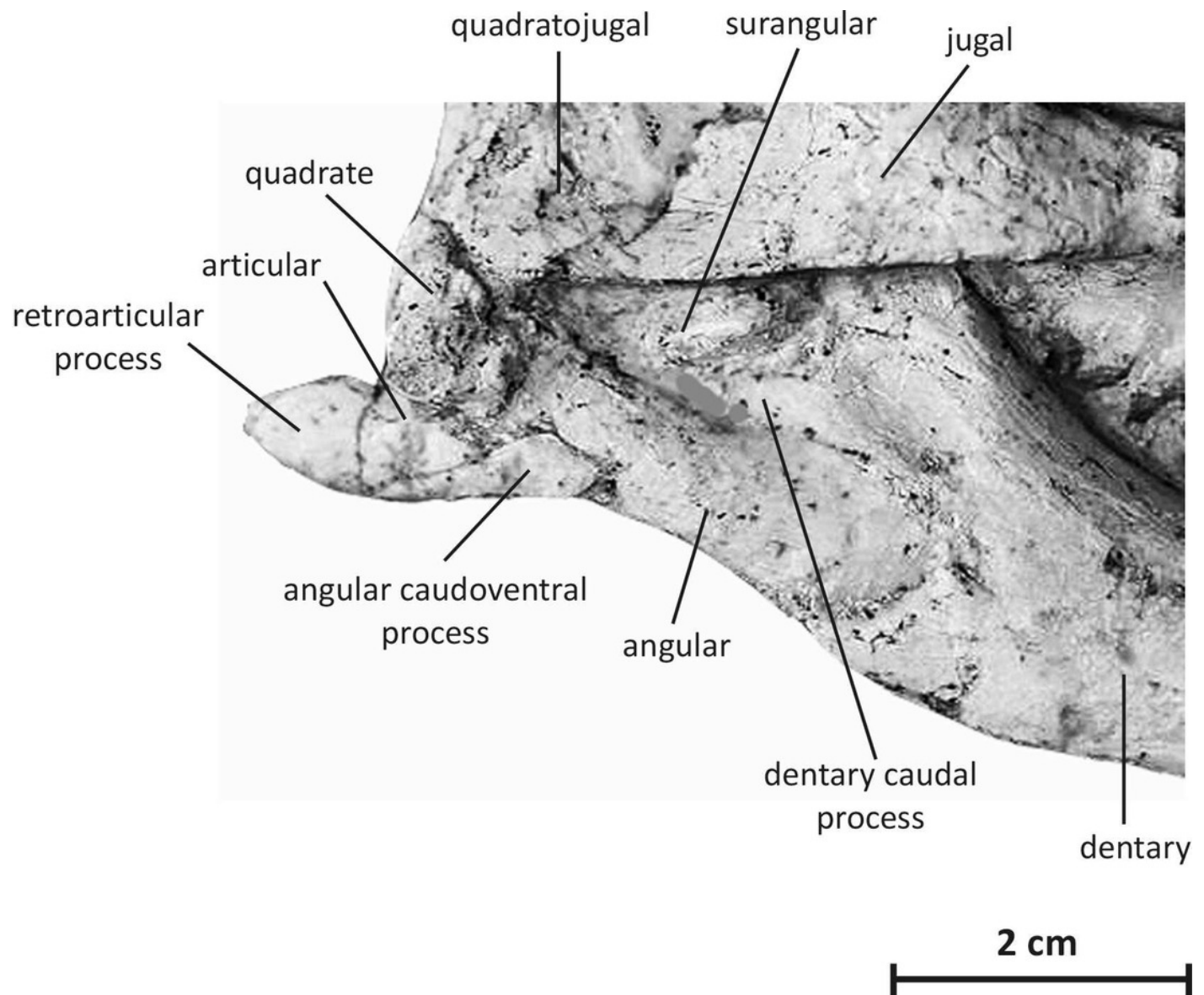


# Figure 8

Axial skeleton of JMOL AD00114.

(A) cervical vertebrae 2 to 4 in right lateral vie; (B) cervical and dorsal series in left lateral view; (C) sacrum and proximal caudal vertebrae in dorsal view; (D) distal caudal vertebrae in left lateral view. Abbreviations: ca: caudal vertebra; cv: cervical vertebra; d: dorsal vertebra.

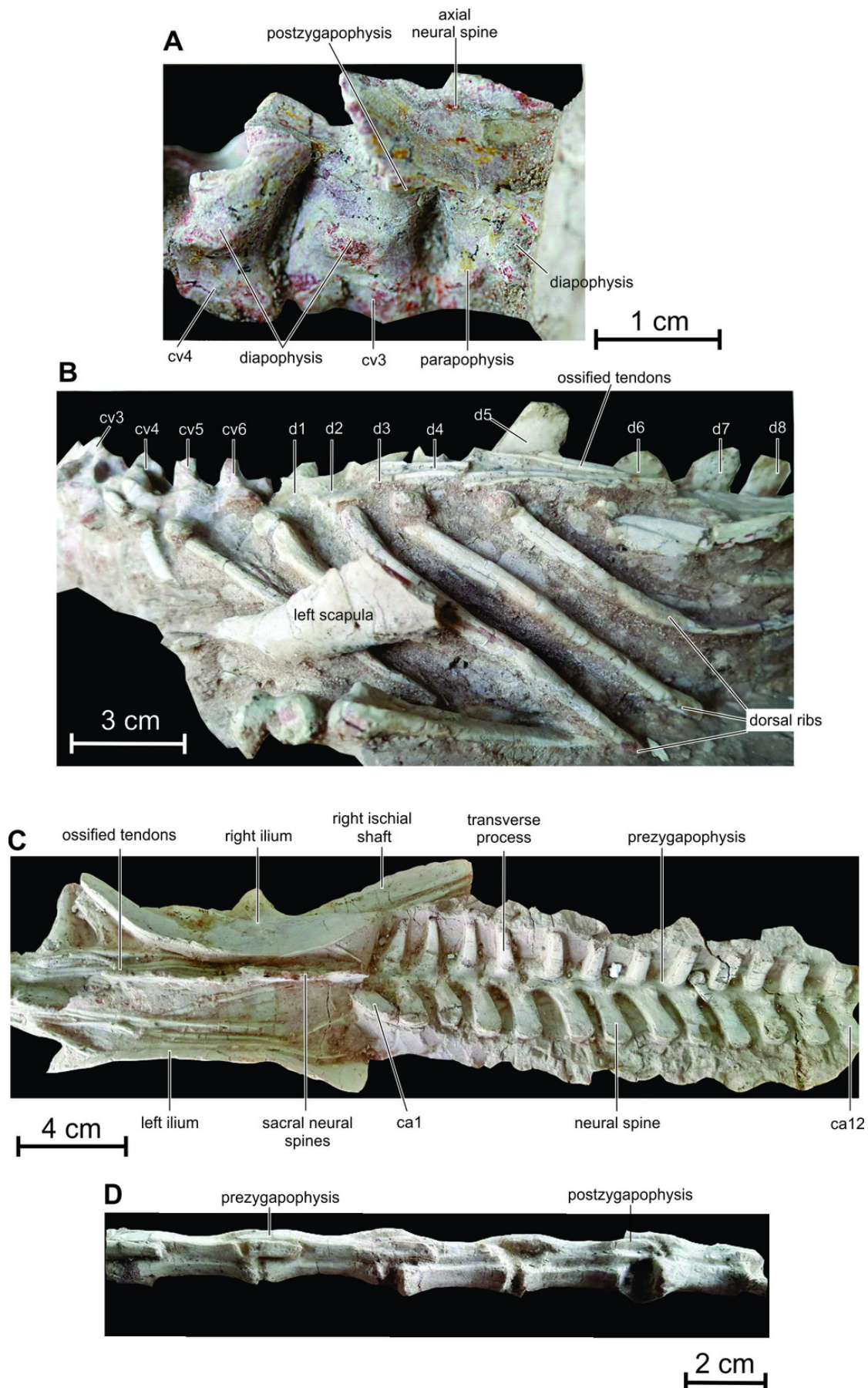


# Figure 9

Right scapular girdle and forelimb of JMOL AD00114.

(A) photograph; (B) line drawing; (C) detail of the right scapulocoracoid in lateral view.

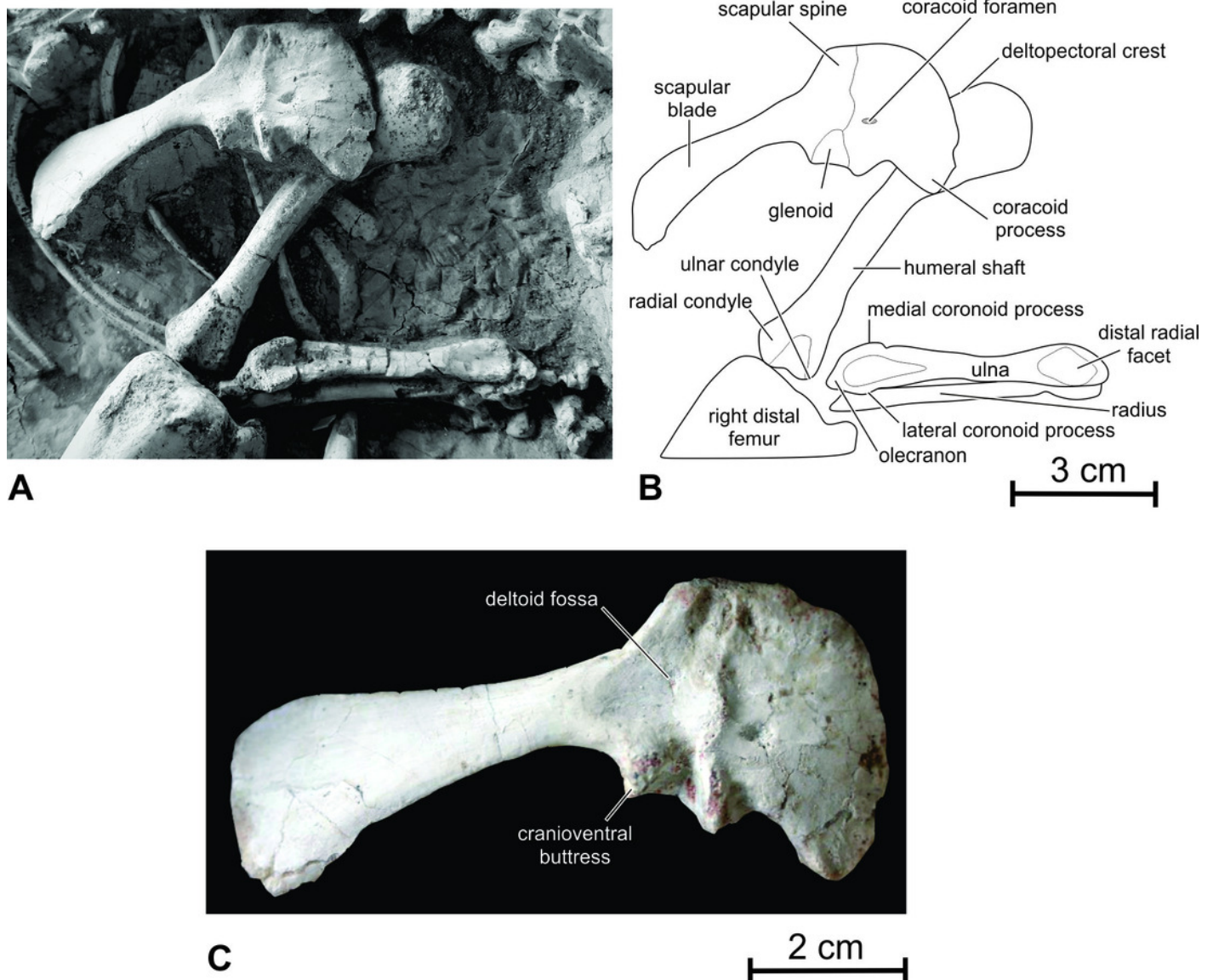




# Figure 10

Pelvic girdle and hindlimbs of JMOL AD00114.

(A) right ilium in lateral view; (B) photograph of distal ischia and right hindlimb; (C) line drawing of distal ischia and right hindlimb; (D) left foot in cranial view; (E) gastroliths.

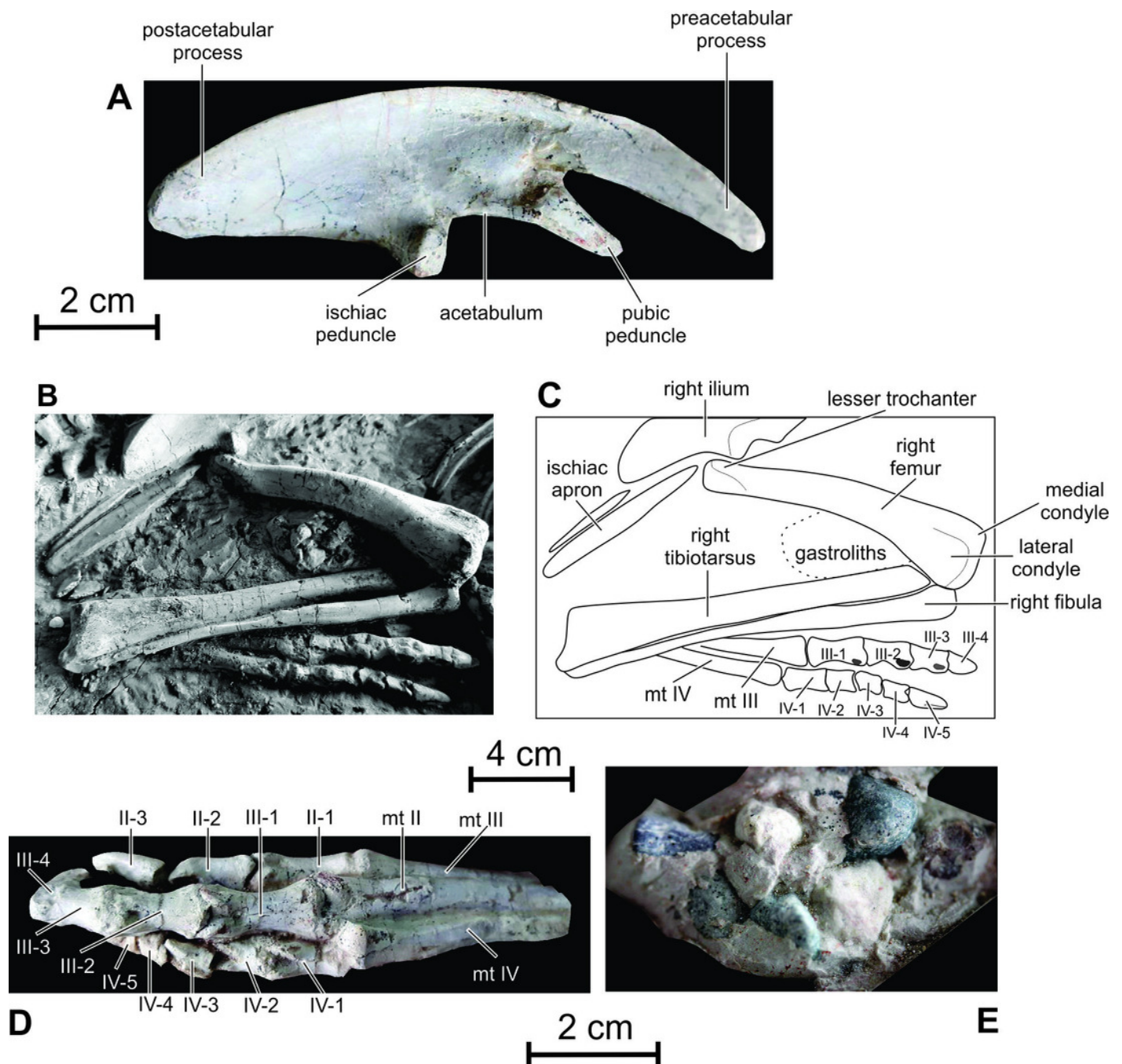


# Figure 11

Phylogenetic position of *Changmiania liaoningensis* gen. et sp. nov. among Ornithischia.

Strict consensus tree of 49 MPT's. Tree Length = 859. Nodal support (Bremer indices > 1) is indicated above or below the branches.



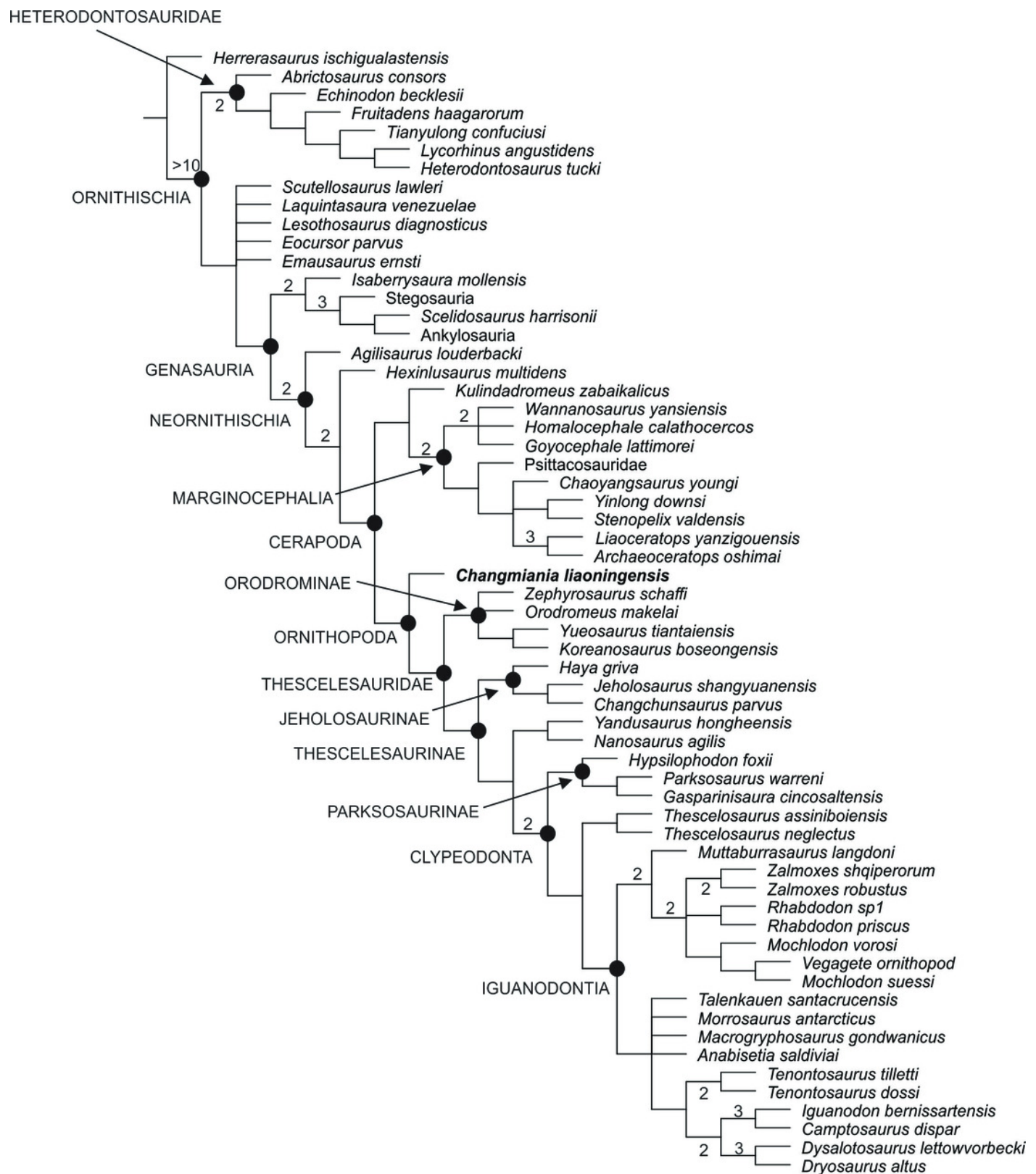


# Figure 12

Phylogenetic position of *Changmiania liaoningensis* gen. et sp. nov. among Ornithischia.

**F**ully-resolved agreement subtree obtained after the exclusion of 5 unstable 'wilcard' taxa, carried out using the 'Comparisons-Agreement subtree(s)' option of TNT (*Goloboff et al., 2008*).

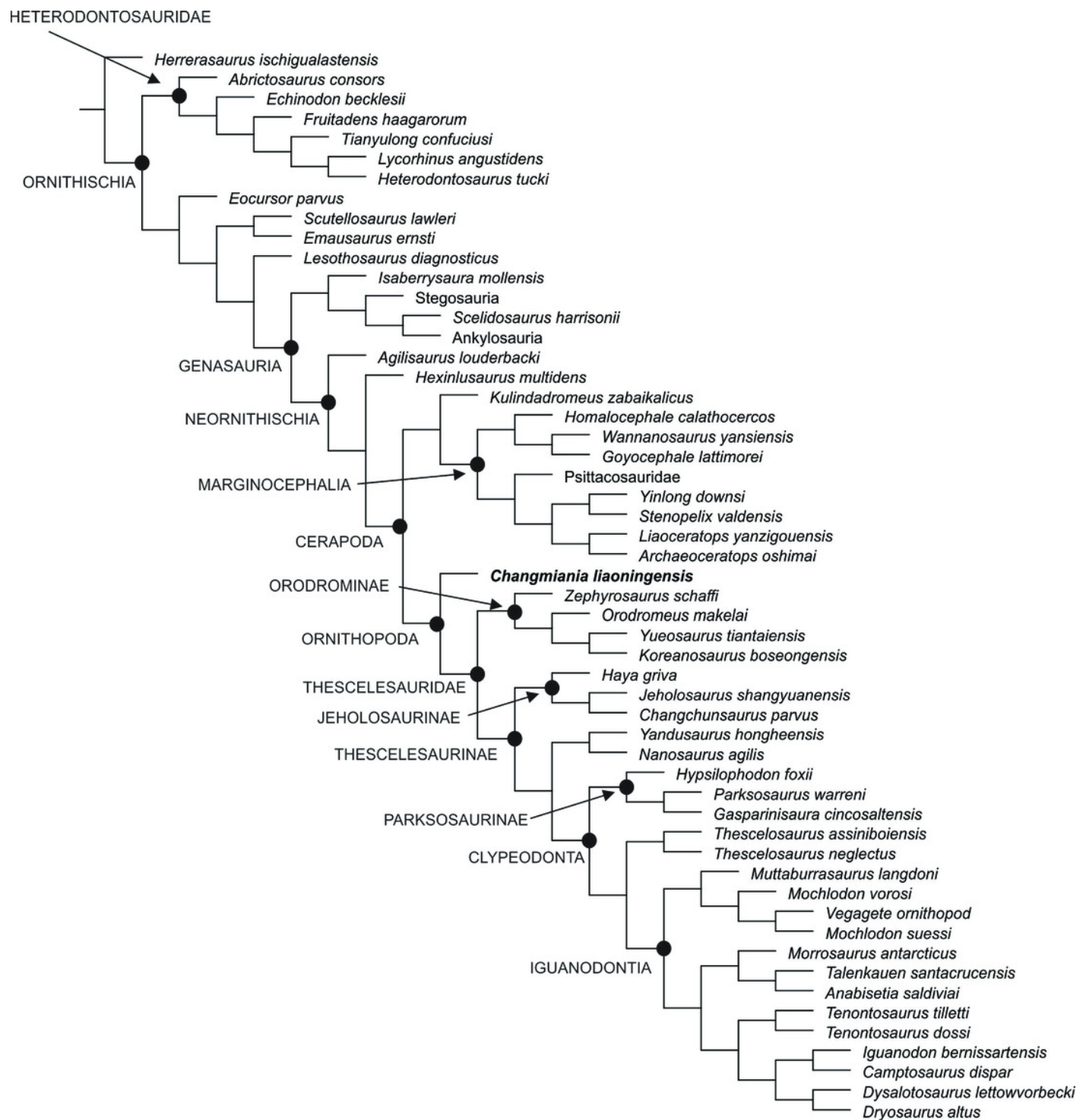


**Table 1** (on next page)

Selected measurements of *Changmiania liaoningensis* JMOL AD00114 specimen.

1		
2	<b>Total length:</b>	1170 mm
3	<b>Skull, length:</b>	110.5 mm
4	maximum height of skull:	37.4 mm
5	<b>Orbit</b> length:	30 mm
6	<b>Snout</b> length:	52 mm
7	<b>External antorbital fenestra</b> length:	13 mm
8	<b>External naris</b> length:	11mm
9	<b>Supratemporal fenestra</b> length:	17 mm
10	<b>Infratemporal fenestra</b> , rostrocaudal length of dorsal margin:	18 mm
11	height:	20 mm
12	<b>Mandible</b> length:	93 mm
13	<b>Dentary</b> , length:	52 mm
14	height of dentary at mid-length:	13.5 mm
15	<b>Tail</b> total length:	650 mm
16	<b>Scapula</b> , length:	68 mm
17	height of proximal head:	27 mm
18	minimum height of blade:	11 mm
19	<b>Humerus</b> , length:	85 mm
20	minimum mediolateral width:	8 mm
21	<b>Ulna</b> , length:	60 mm
22	mediolateral width of proximal end:	11.3 mm
23	mesiolateral width of distal end:	9.3 mm
24	<b>Ilium</b> , length:	101.5 mm
25	length of preacetabular process:	42 mm
26	length of postacetabular process:	36 mm
27	<b>Femur</b> length:	115.5 mm
28	<b>Tibiotarsus</b> length:	140 mm
29	<b>Fibula</b> length:	130 mm
30	<b>Individual pes element lengths:</b>	
31	Mt I: ?   Mt II: ?   Mt III: 67 mm   Mt IV: 60 mm	
32	I-1: ?   I-2: ?	
33	II-1: 19 mm   II-2: 15.2 mm   II-3: 18.4 mm	
34	III-1: 21.5 mm   III-2: 15.6 mm   III-3: 15 mm   III-4: > 20 mm	
35	IV-1: 12.5 mm   IV-2: 12 mm   IV-3: 10.6 mm   IV-4: 10 mm   IV-5: 17.8 mm	





## Table 2 (on next page)

Comparisons of postcranial measurements (in mm) in basal ornithopods: *Changmiania liaoningensis*, *Koreanosaurus boseongensis*, *Hypsilophodon foxii*, *Orodromeus makelai*, and *Oryctodromeus cubicularis*.

**Comparisons of postcranial measurements (in mm) in selected basal ornithopods:** *Changmiania liaoningensis*, *Koreanosaurus boseongensis*, *Hypsilophodon foxii*, *Orodromeus makelai*, and *Oryctodromeus cubicularis*.

1

<b>Taxon</b>	<b>Ref</b>	<b>Humerus length</b>	<b>Femur length</b>	<b>Tibia length</b>	<b>H/F</b>	<b>T/F</b>
<i>C. liaoningensis</i>	JMOL AD00114	85	115.5	140	0.74	1.21
<i>K. boseongensis</i>	KDRC-BB	205-215	196.5	204	> 1	1.04
<i>H. foxii</i>	NHM R5829	159	198	238	0.8	1.20
<i>H. foxii</i>	NHM R5830	74	101	117	0.74	1.16
<i>O. makelai</i>	MOR 294	72	106	132	0.68	1.25
<i>O. cubicularis</i>	MOR 1636	157	-	254	-	-
<i>J. shangyuanensis</i>	IVPP V12542	61.5	94.4	113.4	0.65	1.20
<i>H. griva</i>	IGM 100/2015	86	131	155	0.66	1.18
<i>N. agilis</i>	BYU ESM-163R	104	151	180	0.69	1.19
<i>D. altus</i>	YPM 1876	190	360	395	0.53	1.1

2

3